IEEE Access
Multidisciplinary | Rapid Review | Open Access Journal

Received 3 July 2024, accepted 25 July 2024, date of publication 6 August 2024, date of current version 16 August 2024.

Digital Object Identifier 10.1109/ACCESS.2024.3439344

RESEARCH ARTICLE

Extraction of the Multijunction Solar Cell Parameters Using Two Metaheuristic Algorithms

DANIEL T. COTFAS, MANOHARAN MADHIARASAN, AND PETRU A. COTFAS, (Member, IEEE)
Department of Electronics and Computers, Transilvania University of Brasov, 500036 Brasov, Romania
Corresponding authors: Daniel T. Cotfas (dtcotfas@unitbv.ro) and Manoharan Madhiarasan (mmadhiarasan89@gmail.com)

ABSTRACT The module with multijunction solar cells (MJSC) is an excellent solution for converting solar radiation into electrical energy. Several methods are applied to extract the parameters of the multijunction solar cell. Most of them are analytical and numerical. Metaheuristic algorithms have lately been used for the parameters' extraction. In specialized literature, only a few multijunction solar cells have been performed to extract the parameters. Therefore, two metaheuristic algorithms are proposed in this paper: the Chameleon Swarm Algorithm (CSA) and the Black Widow Optimization Algorithm (BWOA). The first algorithm (CSA) is applied for the first time to estimate the solar cell and panel parameters, and both algorithms (CSA & BWOA) are employed for the first time for the multijunction solar cell. They are applied considering two models: the single diode model (SDM) and the double diode model (DDM) for the multijunction solar cell, and three work temperatures of the multijunction solar cell. Four statistical tests are used to analyze the performance of the algorithms, the main being root mean square error (RMSE). A comparative study was performed using the other analytical and metaheuristic algorithm. The obtained RMSE is 8.9120260701E-5 for BWOA and 8.9123932518E-5 for CSA model, respectively, in the case of SDM model and 41.5°C, 1.0186359636E-4 for BWOA and 1.0088314434E-4 for CSA model, respectively, in the case of DDM model and 41.5°C. In the case of the solar panel the RMSE is 3.62E-3 for BWOA, 3.6250156794E-3 for CSA model, respectively, in the case of SDM model and 25°C. The best root mean square error results are obtained using the Black Widow Optimization Algorithm for the single-diode model. The lowest value for root mean square error is 8.9120260701E-5. The special feature and merits of the proposed algorithms are that they have better exploration and exploitation ability; thus, they provide the optimal results with reduced computational time. Further, the performance of the two algorithms (BWOA andCSA) is validated using the dataset of the CTJ 30 panel. The BWOA algorithm has a root mean square error that is two times lower than the one in the research literature. The computational time is also calculated. It is around 2 s, which is very competitive for all considered cases. CSA has the lowest computing time for all four cases considered, varying from 1.882829 s to 2.277469 s. Furthermore, variation in the temperature function is studied using the extracted parameters.

INDEX TERMS Multijunction photovoltaic cells, parameters, algorithms, one and two diode.

I. INTRODUCTION

Solar and wind energy remain the pillars for renewable energy to reach the net zero emissions target by 2050. The total installed capacity in 2021 for solar photovoltaic energy was 175 GWh, more than 26% compared to 2020. It accounted for over 50% of all installed renewable energy in 2021 [1]. A contribution to this achievement was also brought by new concentrated photovoltaic systems (CPV). Gielen et al. estimate that by 2050, solar energy will represent 25% of the consumed energy and 3% will be produced by CPV systems [2].

The trajectory of the installed capacity of CPV systems is a sinuous one. The installed capacity of CPVs underwent

The associate editor coordinating the review of this manuscript and approving it for publication was Shuo Sun.

a first leap in 2008. It reached 20MWh, and 15 MW of these are in Spain [3]. The year 2012 was a good one; the added installed capacity in CPV was 120 MW, and after that, it reached only 17 MW in 2015 [4]. The installed capacity in CPV significantly increased in 2021, only in China, up to 67.68 MW [5].

Two technologies were used to achieve the CPV: one developed by Amonix, based on monocrystalline silicon, and another developed by Fraunhofer ISE, based on multijunction used in CPV systems, achieved by Concentrix Solar [6]. Nowadays, the CPV is dominated by the multijunction solar cells. Solar cells with triple junctions, as InGaP/InGaAs/Ge, are used in commercial modules, the efficiency being 39.6% at 500 suns and 25°C temperature [7]. Research led to the development of new multijunction solar cells in the laboratory with six junctions and an efficiency of 47.1% at 143 suns [8].

Knowledge of the photovoltaic cell parameters is very important to researchers who aim to improve the performance of the photovoltaic cell so that module manufacturers can achieve the best modules and forecast the energy generated by the photovoltaic modules in different environmental conditions. The majority of the methods and algorithms to extract the PV parameters are taken from other domains [9], [10], and few are developed for the photovoltaic field, such as successive discretization algorithm (SDA) [11] or hybridization HSDA.

In the case of multijunction solar cells, there are two approaches: the first is to consider the single exponential model or single diode model (SDM), which is useful for manufacturers to analyze the behavior in different conditions [12], [13] and forecast the energy production [14] and the second is important for the researchers who work to improve the performance of this solar cell. In this case, it is used for each subcell of the solar cell, the SDM model, and the equivalent circuit is obtained by connecting in series the three equivalent circuits of each subcell [15].

The photovoltaic cells' parameters are extracted using analytical [16], numerical [17], and metaheuristic algorithms, which predict the current-voltage characteristic [18], [19]. Several review papers briefly present, analyze, and compare the methods used to estimate the parameters of photovoltaic cells and panels, as well as PV. Thirty-four methods that allow the estimation from one to five parameters are analyzed in terms of pros and cons [20]. Humada et al. reviewed the papers from research literature, using one and two diodes models, respectively. Additionally, the effect of irradiance and temperature on the estimated parameters is considered [21]. Li et al. approached metaheuristic algorithms from the perspective of statistical tests that provide information about the reliability and robustness of the algorithm. CPU time is also considered in their work to analyze the algorithm's computational resources and time complexity [22]. Twenty-eight metaheuristic algorithms used to extract the PV parameters are quantitatively evaluated, compared, and classified into four categories of algorithms, based on mathematics, biology, physics, and sociology [23]. Datasets for RTC photovoltaic cells and the PWP 201 module are most commonly used to prove the performance of the metaheuristic algorithms [24], [25], [26]. The SDM model is the most widely used to estimate the cell parameters, followed by the double diode model (DDM) [27], [28]. There are several other PV cells and panels used in papers, such as: monocrystalline silicon commercial solar cell, amorphous silicon solar cell, Sharp ND-R250A5, STM6-40, STM6-120, PVM 752 GaAs, Leibold solar module LSM 20 and STE 4/100,1STH-235-WH, HIT-215, S75, ST50, SQ85, KC200GT, SM255, SX3200N, KD210GH-2PU, and ST40 [19], [29], [30], TITAN-12-50 solar panel [31]. Analytical methods and metaheuristic algorithms are rarely applied to multijunction photovoltaic cells [32].

In the following, the state-of-the-art study is focused only on methods and metaheuristic algorithms that extract the parameters of the multijunction solar cells.

The five parameters of InGaP/GaAs/Ge multijunction solar cells were extracted using the Newton–Raphson method and the SDM model. In the case of non-uniform illumination, the equivalent circuit for the SDM model is improved with a term that considers the behavior of the diode avalanche; in this case, eight parameters are calculated. A statistical test, least square error, or the predefined number of iterations is used to end the iterative process. The values for the statistical test obtained through Newton–Raphson method vary from 1.95E-6 for 350 concentration ratio to 4.8E-6 for 900 respectively [15].

Appelbaum and Peled compare three methods, namely the Newton-Raphson method, Levenberg–Marquardt method, and the Genetic algorithm, to extract the multijunction solar cell parameters using the SDM model, for three concentration ratios: 350, 555, and 750 suns [33]. The statistical test used for comparison is calculated as a ratio between the sum of the squared differences between measured and calculated currents, and the sum of squared measured currents [33]. There is no best method, so for 350 suns, the best results are given by the Genetic algorithm; for 555 suns, the best is the Levenberg–Marquardt method; and for 750 suns, the best is the Newton-Raphson method.

Fernández et al. applied four methods to extract the multijunction solar module parameters under concentration lights. The modules have twenty GaInP/GaInAs/Ge solar cells connected in series [34]. Three of the four methods applied are analytical and are proposed by Phang et al. [35], Blas et al. [36], and Khan et al. [37] based on the experimental values of the short circuit current (I_{sc}), open circuit voltage (V_{oc}), and the coordinates of the maximum power point (P_{max}), (V_{max} and I_{max}). Also, the first values of the series and shunt resistance are found in the experimental current-voltage characteristic. The fourth method is numerical and uses five current-voltage characteristics for five points with the voltage 0, Vmax, V_{oc}, $V_{oc}/2$, and the average between V_{max} and V_{oc} to obtain a system with five equations. It was developed

by Almonacid et al. [38]. Two statistical tests are applied to compare the four methods (Phang, Almonacid, Blas, Khan): RMSE and mean bias error (MBE). The results for RMSE are: 1.22%, 1.35%, 1.71%, and 3.53%. For MBE, the results are: −0.46%, −0.40%, −0.66% and −1.81%. The best results are obtained using Phang's and Almonacid's methods.

Romero et al. analyzed the GaInP/GaInAs/Ge multijunction panel, which consists of 25 cells connected in series, under 550 suns concentration. The methods used for the extraction of the parameters are Phang, Blas, and Khan. The performance of the methods is analyzed using the normalized RMSE (NRMSE) and MBE. The best method was developed by Phang, where NRMSE was 1.55%, and MBE was −0.41% [32].

Two CPV modules, by GaInP/GaInAs/Ge solar cells, are tested at different concentration rates to analyze the behaviour of the parameters in function of the irradiance level. The parameters are extracted using the method developed by Phang and the SDM model [17]. The analysis shows that if the irradiance increases, the photogenerated current (I_{ph}) has a linear increase, the series resistance (R_s) and the shunt resistance (R_{sh}) decrease, and reverse saturation current (I_{o1}) and ideality factor of diode (n) remain almost constant [17].

Three methods to extract the parameters of the multijunction solar cell ($In_{0.49}Ga_{0.51}P/In_{0.01}Ga_{0.99}As/Ge$) using the SDM model and for each subcell are compared for two levels of irradiance, one sun and 350 suns [39]. The first method used is Blas [36], the second is developed by Xiao et al. [40], who considered that the shunt resistance is very high and it can be neglected from the SDM model, and the third is a Generalized reduced gradient algorithm based on the tool with the same name from Microsoft Excel [40]. Three statistical tests are used to compare the methods considered: mean absolute percentage error, the determination coefficient, and the absolute error at the maximum power point. These are applied for each subcell and for the entire cell. The values obtained are 1.2313, 0.9746 and 8.3527E−12 using the Blas method and 0.0094, 0.9999 and 2.5899E−07 for Xiao method [40].

Singh et al. use the Lambert W-function to extract the parameters of each subcell of the multijunction solar cell [41]. Muhammadsharif developed a new method to extract the parameters of the CTJ30 multijunction solar cell, using the SDM model and the new simplified method (SM). It is an iterative method, and firstly, it calculates the n and R_{sh} from the maximum of the function f(n, R_{sh}) = n(R_{sh_max} - R_{sh}). These values are used to calculate the other three parameters [42]. The average relative error calculated for the CTJ30 dataset is 2.86%. This proves a good match between the dataset values and those calculated using the method, and only a small deviation appears for the maximum power point [42].

Rezk and Fathy proposed using the Water Cycle Algorithm (WCA) to extract parameters for each subcell of the InGaP/InGaAs/Ge multijunction solar. The current-voltage characteristics are obtained using Matlab software. It is considered a solar module with 20 solar cells connected in series [43]. For this, five metaheuristic algorithms are applied: WCA, harmony search algorithm (HAS), grey-wolf optimizer algorithm (GWO), mine blast algorithm (MBA), and antlion optimizer algorithm (ALO) [43]. The best results are obtained by the WCA algorithm, proved by statistical tests applied such as RMSE, MAE and integral time absolute error, ITAE. The values obtained are 2.347791 for RMSE, 0.974546 for MAE and 0.020506 for ITAE.

Ghani et al. developed a new method to extract the parameters of the multijunction solar cell (GaInP1.88/GaInAs1.41/Ge0.67) with an area of 0.765 cm^2 based on the multivariable Newton-Raphson method. The RMSE calculated for the maximum power is compared with that obtained by Almonacid, Blas and Khan. There is an improvement in the Ghani method compared with Khan, 56%, and 34% compared to Blas. The Almonacid method outperforms the Ghandi method with 7% [44]. Nouri et al. developed a method to extract the five parameters of the InGaP/GaAs/Ge multijunction solar cell based on the single diode model [45].

As the state-of-the-art study on extracting the parameters of the multijunction solar cell shows, there are numerous analytical and numeric methods, but few metaheuristic ones. The last ones demonstrate the ability to extract the parameters of the photovoltaic cells and panels accurately [30], [46]. This work proposes two powerful and recent metaheuristic algorithms to cover this gap. The algorithms are used to extract the parameters for the multijunction solar cell manufactured by SolAero InGaP(1.86eV)/InGaAs(1.40eV)/Ge(0.67eV), area 1 cm^2 and to validate the results they are also applied for CTJ30 solar cell, area 26.5 cm^2, for CESI.

Another limitation for the study of the multijunction photovoltaic cells or panels is the existence of very few datasets in research literature, while for the photovoltaic cells with homo and hetero junctions or for the photovoltaic modules there are many [26], [47]. Therefore, this paper provides three datasets for multijunction photovoltaic cells, each corresponding to different irradiances and temperatures.

To simplify the complexity of the equivalent circuit of the multijunction and reduce the time required to extract the parameters, as well as to study the behavior of the cell based on environmental parameters to forecast energy production, the SDM model is utilized [12], [48], [49]. This approach is analyzed in the paper.

The novelty and the significant contributions are:

- Chameleon Swarm Algorithm (CSA) is adapted and implemented to extract the parameters of the multijunction solar cell (MJSC) for the first time.
- Black Widow Optimization Algorithm (BWOA) is used for the first time to extract the parameters of the multijunction solar cell. It was used with success for other photovoltaic cells and panels.
- Three data sets are measured for InGaP/InGaAs/Ge multijunction solar cell at three different temperatures; The researchers can use the datasets from the Supplementary files to achieve comparisons between the results

obtained in this paper and those will be obtained with other metaheuristic algorithms or methods.
- The results obtained by the two algorithms are compared using four statistical tests: the root mean square error (RMSE), the mean absolute error (MAE), the coefficient of determination (R^2) and the t-statistic (t-stat).
- The algorithms are applied to compare the usual single-diode model and the double-diode model, determining which model is more appropriate.
- The two algorithms are applied to a dataset from the specialized literature for comparison in RMSE and the comparison with SM method shows the superiority of the BWOA and CSA algorithms.
- The variation of the parameters calculated for the SDM model in function of temperature is made.

The second section describes the SDM and DDM models and the two algorithms. The results are analyzed in the third section of the paper. The conclusion and future work are shown in the last section.

II. MODELS AND METHODS

A. MJSC MODELS

Two models are used to analyze the multijunction solar cell SDM and DDM models. The most model utilized in specialized literature is the SDM model due to its simplicity and ease of implementation in analytical or numerical methods. Also, these advantages are kept for the implementation of the metaheuristic algorithms. This model is used in several papers to extract the parameters of multijunction photovoltaic cells and analyze their behavior [12], [15], [33]. The equivalent circuit for the SDM is presented in Fig.1a, and the mathematical model is in (1) [19], [50]. The DDM model is more complex. Recently, it was successfully applied to many solar cells and panels. It considers both mechanisms that take place in solar cells: diffusion, generation, and recombination, respectively. Fig.1b shows the equivalent circuit for the DDM model, and (2) describes the mathematical model [19].

$$I = I_{ph} - I_{o1}\left(e^{\frac{V+IR_s}{n_1 V_T}} - 1\right) - \frac{V+IR_s}{R_{sh}} \tag{1}$$

$$I = I_{ph} - I_{01}\left(e^{\frac{V+IR_s}{n_1 V_T}} - 1\right) - I_{o2}\left(e^{\frac{V+IR_s}{n_2 V_T}} - 1\right) - \frac{V+IR_s}{R_{sh}} \tag{2}$$

where, $V_T = kT/q$, $q = 1.60217646E\text{-}19C$ is the electric elementary charge, $k = 1.3806503E\text{-}23J/K$ is Boltzmann constant, and T represents the temperature of the multijunction solar cell, the index 1 and 2 shows the mechanisms of diffusion, and generation and recombination respectively.

B. ALGORITHMS

Two algorithms, namely the Black Widow Optimization Algorithm, and Chameleon Swarm Algorithm, were used to extract InGaP/GaAs/Ge multijunction solar cell parameters. The two algorithms are described below.

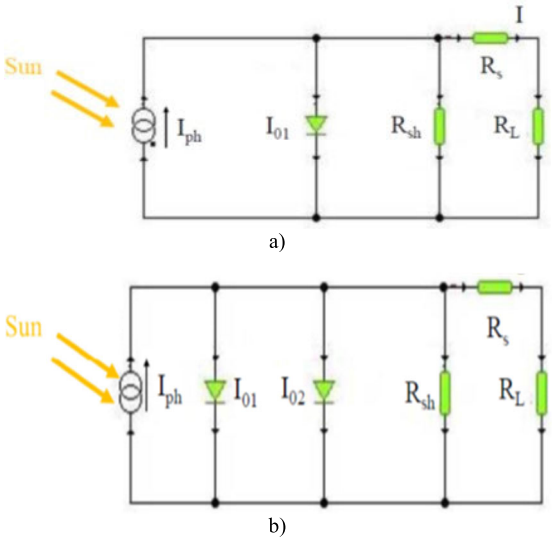

FIGURE 1. MJSC equivalent circuits: a) Single diode model; b) Double diodes model.

1) BLACK WIDOW OPTIMIZATION ALGORITHM (BWOA)

Hayyolalam and Kazem 2020 devised a Black Widow Optimization Algorithm with inspiration from Black Widow Spider Mating Behavior [51]. Peña-Delgado et al. [52] employed the Black Widow Optimization Algorithm to selectively eliminate harmonics in a three-phase eleven-level inverter. Nouri et al. [45] applied the Black Widow Optimization Algorithm (BWOA) for the calculation of various PV cell/Panel parameters. The detailed description of the BWOA algorithm refers to our previously published paper [53], which describes the workflow and procedure process depicted as a flowchart in Fig. 2.

The mathematical modelling of the BWOA is as follows:

Movement: The spider's movements inside the web were classified as linear and spiral, as shown in (3) [51].

$$\vec{S}_i(n+1) = \begin{cases} \bar{S}_{best}(n) - q\vec{S}_{r_1}(n) \\ \qquad if\ rand() \le 0.3 \\ \bar{S}_{best}(n) - \cos(2\pi\delta)\vec{S}_i(n) \\ \qquad for\ other\ circumstance \end{cases} \tag{3}$$

where, $\vec{S}_i(n+1)$-the new position of a search agent, q-the randomly generated float number between $[0.4,\ 0.9]$, $\vec{S}_{r_1}(n)$ - position of the r_1 search agent with $i \neq r_1$, $\vec{S}_{best}(n)$ the previous iteration best search agent, "r_1 varies between 1 and the maximum size of search agents generated by a random integer number, $\vec{S}_i(n)$ - the position of the current search agent, δ-the randomly generated float number in the interval $[-1.0, 1.0]$" [53].

The q and δ fluctuates between the range $-1.0 \le \delta \le 1.0$ and $0.4 \le q \le 0.9$ randomly for each iteration. The value of q and δ underlying reason for the linear and spiral movement, respectively.

Pheromones: Pheromones play an important role in spider mating. A female spider having low pheromone rates implies

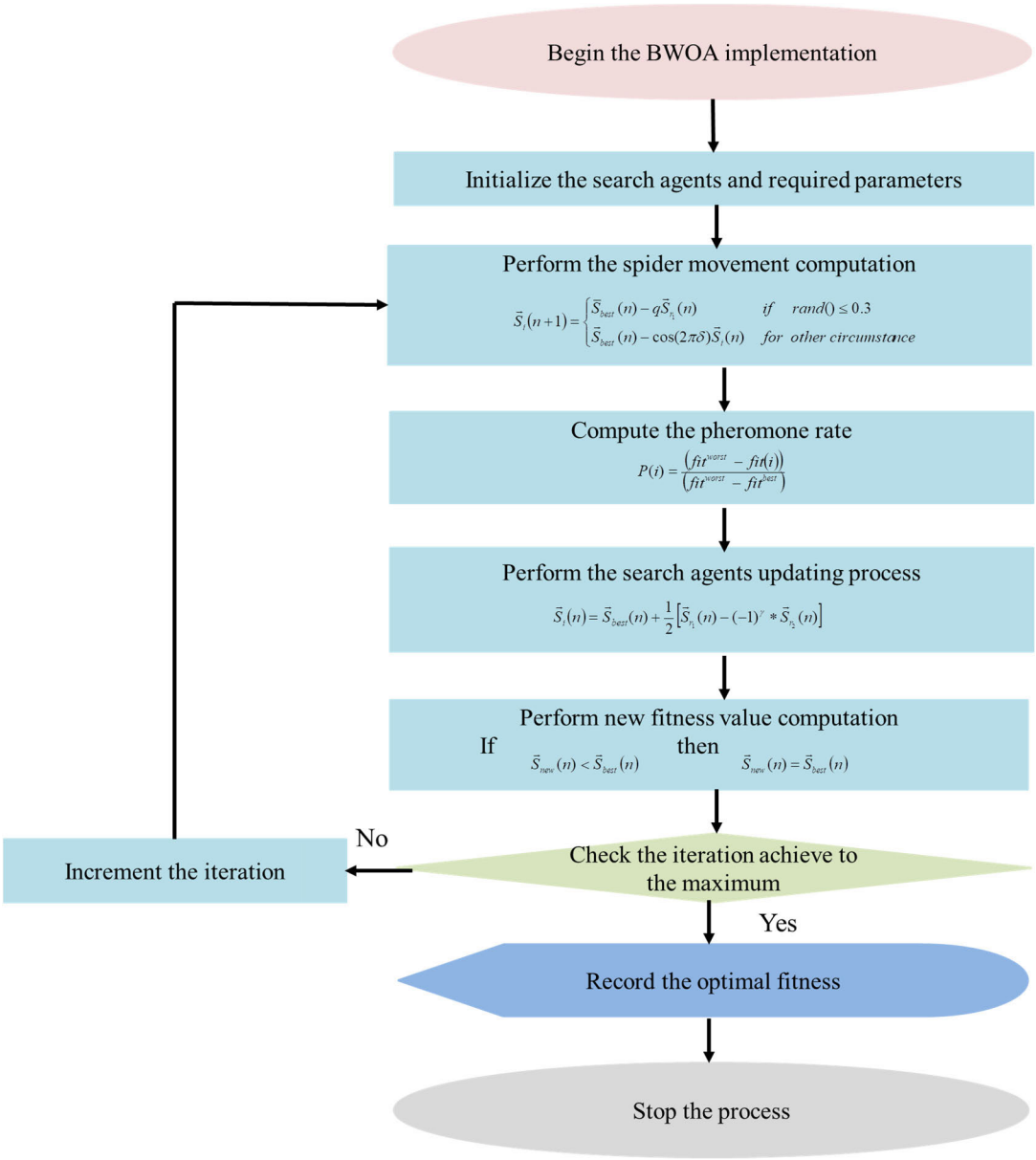

FIGURE 2. Workflow and procedure process of BWOA [45].

a starving cannibal spider. Male spiders do not usually choose female spiders that have low pheromone rates. Another female spider would be substituted for low pheromone rates, ratings of 0.3 or lower.

$$P(i)=\frac{\left(fit^{worst}-fit\ (i)\right)}{\left(fit^{worst}-fit^{best}\right)} \tag{4}$$

where $fit(i)$- the i^{th} search agent's current fitness value, fit^{worst}- the current generation best fitness value, fit^{worst}- the current generation worst fitness value.

The search agent has been updated using the following formulation.

$$\vec{S}_i\ (n)=\vec{S}_{best}(n)+\frac{1}{2}\left[\vec{S}_{r_1}(n)-(-1)^{\gamma}*\vec{S}_{r_2}(n)\right] \tag{5}$$

where γ represents a randomly generated binary number, $\gamma \in \{0, 1\}$, "r_1, and r_2 are random integer numbers derived between 1 and the maximum size of search agents, provided $r_1 \neq r_2$, $\vec{S}_i\ (n)$ is the low pheromone rate search agent is going to be modified, $\vec{S}_{r_1}\ (n)$, $\vec{S}_{best}\ (n)$ is best past iterations best search agent, $\vec{S}_{r_2}\ (n)$- r_1, r_2 chosen search agents" [53].

The new fitness value ($\vec{S}_{new}\ (n)$) is a new search agent.

$$If\ \vec{S}_{new}(n) < \vec{S}_{best}\ (n)\ \ then\ \vec{S}_{new}(n)=\vec{S}_{best}\ (n) \tag{6}$$

2) CHAMELEON SWARM ALGORITHM (CSA)

Chameleon Swarm Algorithm is inspired by chameleons' typical foraging activity and their made progress in foraging

for food in desert areas and jungles, which was developed by Braik in 2021 [54]. Both exploration and exploitation are critical components of every meta-heuristic algorithm's effectiveness, algorithms must be efficiently built to achieve an appropriate balance between exploration and exploitation. The capacity of optimization algorithms to globally explore diverse sections of the search space is referred to as exploration. It is thus essential to mitigate the impact of local optima and the migration out of local optima stagnation. Exploitation is the ability to look for prospective solutions locally throughout all important sectors to boost solution quality.

A systematic way to develop innovative meta-heuristics is to demonstrate their effectiveness in tackling optimization issues compared to traditional approaches and other meta-heuristics. It is essential to emphasize that it is not feasible to propose an algorithm that can find global solutions to all types of issues. Chameleons use their globular eyes to scan a vast radius of search and exploit every available location in the search zone. During hunting, Chameleons use their incredibly sticky and lengthy tongues to catch prey quickly and efficiently. Proposed an adjustable parameter throughout Chameleon Swarm Algorithm iterations to help Chameleons better explore the solution space to accomplish an improved balance of exploration and exploitation for further dependable performance.

Chameleons are adapted to climbing and visual hunting and have remarkable eyesight that allows them to visualize up to 32 feet ahead of themselves. It thus simplifies the process of finding prey. Chameleons deploy their capacity to change colours to fit their circumstances to defend themselves when an offender is around. In reality, the hunting activity of chameleons and their successful tactics of locating, chasing, and catching prey inspired the mathematical models established in this study to build CSA and conduct optimization.

The following are the major phases of a chameleon pursuing prey:

1. Locating the prey: Chameleons travel the territory and forests looking for prey, and their location alters as a response.

2. Chasing prey using its eyes: Both eyes may exist simultaneously to rotate and concentrate on the location of prey at the same instant. Eyes work together to focus forward, giving a binocular vision of prey. Thus, it provides chameleons with an entire 360° viewing area around their bodies with 180 degrees along each side; they are able to view everything surrounding them. Then, if a chameleon detects prey, two eyes can focus on the same location for good aim. It spins and goes to the prey's location.

3. Catching the prey: Chameleons mostly eat by capturing prey with sticky tongues.

3) MATHEMATICAL MODELLING OF CSA

The CSA algorithm is developed from the inspiration of chameleons locating the prey, chasing the prey, catching prey behavior, and its mathematical modelling, which are significant processes described as follows.

Initialization and function assessment: Every chameleon is a potential solution to a problem and may be described in a two-dimensional C matrix with size where, m - chameleon population, i - search space dimension. The formulation (7) vector can indicate the chameleon's location in the solution space at iteration [54].

$$C_i^c = \left[C_{i,1}^c, C_{i,2}^c, C_{i,3}^c, .., C_{i,x}^c\right] \tag{7}$$

let = 1, 2,. . . ,m, i denotes the current iteration, x represents the problem dimension, and $C_{i,x}^c$ is the location of the c^{th} chameleon at the x^{th} dimension.

Equation (8) represents the generation of the initial population [54].

$$C^c = L_x + rn \times (U_x - L_x) \tag{8}$$

In which C^c is the c^{th} chameleon's beginning vector, L_x and U_x are the lower and upper boundaries of the exploration region in the x^{th} dimension, and rn is a uniformly generated random value between 0 and 1.

Based on a fitness function, the effectiveness of the outcome is evaluated for each new location of a chameleon. If the outcome effectiveness of the new location is better than the outcome effectiveness of the current one, the current location is updated. Interestingly, the chameleons in the Chameleon Swarm Algorithm maintain their present place if their outcome effectiveness is superior to the new location.

a: LOCATING THE PREY

The location update approach may be used to numerically simulate chameleon movement while hunting [54].

$$C_{i+1}^{c,x} = \begin{cases} C_i^{c,x} + u_1\left(BL_i^{c,x} - GB_i^x\right) rn_2 + u_2\left(GBL_i^x - C_i^{c,x}\right) \\ \qquad rn_1 rn_i \geq P^p \\ C_i^{c,x} + \alpha\left(\left(U^x - L^x\right) rn_3 + L_a^x\right) \operatorname{sgn}(rand - 0.5) \\ \qquad rn_i < P^p \end{cases} \tag{9}$$

where $C_{i+1}^{c,x}$ is the c^{th} chameleon's new location in the x^{th} dimension in the $(i+1)^{th}$ iteration phase, $C_i^{c,x}$ is c^{th} chameleon's current location in the x^{th} dimension in the i^{th} iteration phase, $BL_i^{c,x}$ is the best location that c^{th} chameleon obtained yet in the x^{th} dimension at iteration cycle i, GBL_i^c is any of the chameleon's global best locations in the x^{th} dimension determined yet in the i^{th} iteration, u_1 =0.25 and u_2 =0.50 - both are positive values that govern the ability to explore, rn_1, rn_2,rn_3- are uniformly obtained random numbers between 0 and 1, rn_i- a uniformly obtained random number at index i between 0 and 1, P^p is the probability of the chameleon identifying prey = 0.1, $sgn(rand - 0.5)$ is influences the course of both exploration and exploitation and may be a value of 1 or −1, α - as observed in formulation (10), it's a parameter specified as a function of iterations that decreases with the number of iterations.

$$\alpha = \mu_3 e^{\left(\mu_1 i/I\right)^{\mu_2}} \tag{10}$$

where, α is the function of iteration decay with (α), μ_1=*1*, μ_2=*3.5*, μ_3=*3* - constant value control exploration and exploitation.

b: CHASING PREY USING ITS EYES

Chasing prey using its eyes, the following procedures are suggested.

- Redirect the chameleon's initial location to the center of gravity (i.e., the origin).
- Locate the rotation matrix that determines the prey's location.
- Update the chameleons' location using the rotation matrix at the center of gravity, and lastly.
- Redirect the chameleons returning to their original location.

The following mathematical formulation can be utilized to update a chameleon's new location:

$$C_{i+1}^{c} = CR_i^c + \bar{C}_i^c \tag{11}$$

were C_{i+1}^{c}- following rotation, a chameleon's new location, CR_i^c- the center of the chameleon's current location prior to rotation, $\bar{C}_i^c$- the chameleon's rotating centered coordinates in search space.

$$CR_i^c = RM \times CC_i^c \tag{12}$$

where CC_i^c- iteration i centering coordinates, RM - a rotation matrix corresponding to a chameleon's rotation.

$$CC_i^c = C_i^c - \bar{C}_i^c \tag{13}$$

where C_i^c-the chameleons' current location at iteration i.

$$RM = A\left(\varphi, \vec{V}_{\vec{k}_1,\vec{k}_2}\right) \tag{14}$$

where A - rotation matrices in the corresponding axes, ϕ - Chameleon rotation angle, $\vec{V}_{\vec{k}_1,\vec{k}_2}$-two orthonormal vectors in the m-dimensional search space with $x \times 1$ vector size

$$\varphi = rn_4 \text{sgn}(rand - 0.5) \times 180^\circ \tag{15}$$

where rn_4- the random number in the range [0, 1] is generated for establishing a rotation angle ranging from 0 degrees to 180 degrees, *sgn(rand – 0.5)* - the rotational direction to be either 1 or 1.

The rotation matrices in tandem with the X and Y axes in three dimensions are as follows [54]:

$$RM^X = \begin{bmatrix} 1 & 0 & 0 \\ 0 & \cos\omega & -\sin\omega \\ 0 & \sin\omega & \cos\omega \end{bmatrix} \tag{16}$$

$$RM^Y = \begin{bmatrix} \cos\tau & 0 & \sin\tau \\ 0 & 1 & 0 \\ -\sin\tau & 0 & \cos\tau \end{bmatrix} \tag{17}$$

where ω - the rotational angle pertaining to the X- axis, τ -the rotational angle pertaining to the Y - axis.

Catching the prey: The chameleon that goes most near to the prey is meant as the best, as it is optimal. To chase prey, the chameleon utilizes its tongue. As a result, its location is a bit modified as it may lower its tongue twice its length.

Using (18), the velocity of a chameleon's tongue is computed [54]:

$$CTV_{i+1}^{c,x} = \varepsilon\, CTV_i^{c,x} + p_1\left(CGBL_i^{c,x} - C_i^{c,x}\right) rp_1 + p_2\left(CBL_i^{c,x} - C_i^{c,x}\right) rp_2 \tag{18}$$

where $CTV_{i+1}^{c,x}$- the c^{th} chameleon's new velocity in the x^{th} dimension at iteration i+*1*, $CTV_i^{c,x}$- the c^{th} chameleon's current velocity in the x^{th} dimension at iteration i, $C_i^{c,x}$-the c^{th} chameleon's current location, $CBL_i^{c,x}$-the c^{th} chameleon's best-known location, $CGBL_i^{c,x}$- best global location obtained yet by the chameleons, p_1, p_2 - constant value equal to 1.75 and 1.75 respectively, it controls the effect of $CBL_i^{c,x}$ and $CGBL_i^{c,x}$ on the chameleon's tongue dropping, rp_1, rp_2 -two random numbers dispersed between 0 and 1, ε - the inertia weight that decreases linearly with successive iterations as shown in (19), it enhancing CSA convergence behavior.

$$\varepsilon = \left(1 - {}^{i}/_{I}\right)^{\left(\sqrt[rp]{i/I}\right)} \tag{19}$$

where rp - positive value equal to one, employed to regulate exploitation ability, i,I - current and maximum number of iterations.

$$\sigma = 2590 * (1 - e^{-\log(i)}) \tag{20}$$

The chameleon's location, which can be calculated using the third equation of motion as follow [42],

$$C_{i+1}^{c,x} = C_i^{c,x} + \left(\left(CTV_i^{c,x}\right)^2 - \left(CTV_{i-1}^{c,x}\right)^2\right)/_{(2\sigma)}. \tag{21}$$

where, $CTV_{i-1}^{c,x}$-the cth chameleon's previous velocity in the x^{th} dimension, σ - the rate at which the chameleon's tongue projection accelerates, which is defined in (20).

To resemble the hunting habits of chameleons, (9), (11), and (17) were presented.

4) CSA PROCEDURES

The Chameleon Swarm Algorithm (CSA) procedure process is as follows,

Procedure 1: Perform the parameter initialization of all required variables of CSA

Procedure 2: Compute the rotating centered coordinates of the chameleon using Eq. (12)

Procedure 3: Initialize the chameleon in the search space using Eq. (8)

Procedure 4: Initialize the velocity of chameleon tongues

Procedure 5: Compute the location of the chameleon

Procedure 6: Compute the Eqs. (10), (19), and (20)

Procedure 7: Locating the prey using Eq. (9)

Procedure 8: Update the new location using Eq. (11)

Procedure 9: Perform the catching the prey process

Procedure 10: Compute the chameleon tongue velocity using Eq. (18), and location using Eq. (21).

Procedure 11: Based on the upper and lower bound modifies the chameleon location

Procedure 12: Compute and update the chameleon's new location

Figure 3 depicts the workflow and procedural process as a flowchart. Figure 4 depicts the generalized workflow of the multijunction solar cell parameters extraction for both algorithms.

III. RESULTS AND DISCUSSIONS

The InGaP/InGaAs/Ge multijunction solar cell with 1cm/1cm (1 cm^2 area) was measured at one sun irradiance at three temperatures 41.5°C, 51.3°C, and 61.6°C. The measurements were made in natural sunlight using the RELab system which is described in [55]. The two algorithms use the datasets, voltage current pairs (V,I), for each temperature to extract the five or seven parameters of the MJSC considered. The five analytical parameters method, 5P, was implemented [56], in the case of the SDM model, to extract the parameters of the multijunction solar cell and to compare the results with those obtained by the BWOA and CSA algorithms. The performance of the algorithms is analyzed using four statistical tests, presented by the following equations 22-26. First is the root mean square error (22):

$$RMSE = \sqrt{\frac{\sum_{i=1}^{p} (I_{ic} - I_{im})^2}{p}} \tag{22}$$

where, p is the number of the V,I pairs, I_{ic} and I_{im} are the currents calculated and measured respectively, and X is the vector of the parameters, with five parameters for the SDM model and seven for the DDM model, respectively. The RMSE must be minimized.

The second is the mean absolute error (23):

$$MAE = \frac{\sum_{i=1}^{n} |I_{ic} - I_{im}|}{n} \tag{23}$$

The third is the coefficient of determination, (24), which shows the matching between calculated and measured points:

$$R^2 = 1 - \frac{\sum_{i=1}^{n} (I_{ic} - I_{im})^2}{\sum_{i=1}^{n} \left(I_{im} - \overline{I_{im}}\right)^2} \tag{24}$$

The fourth is the t-statistic, (25), which shows the performance of the algorithm. The smaller the value of t-stat, the better the algorithm's performance.

$$t - stat = \sqrt{\frac{(n-1)\, MBE^2}{RMSE^2 - MBE^2}} \tag{25}$$

where MBE is mean bias error.

To optimize the parameters extraction of the multijunction solar cells, it is necessary to minimize the errors between the calculated with the metaheuristic algorithms and the measured values. The objective function established to check the consistency of the algorithms is given by (26).

$$RMSE\ (v) = \sqrt{\frac{\sum_{i=1}^{p} (f(V, I, v))^2}{p}} \tag{26}$$

TABLE 1. Parameters intervals for both models.

Models	I_{ph} [A]	I_{o1} [A]	n_1	R_s [Ω]	R_{sh} [Ω]	I_{o2} [A]	n_2
SDM	0.001-0.2	E-40 – E-05	1–4	0.001-3	0-100000		
DDM	0.001-0.2	E-40 – E-05	1–4	0.001-3	0-100000	E-40 – E-05	1–4

where v represent the parameters vector for each model, $v_{SDM} = (I_{ph}, I_{o1}, n_1, R_s, R_{sh})$ and $v_{DDM} = (I_{ph}, I_{o1}, I_{o2}, n_1, n_2 R_s, R_{sh})$), f(V,I,v) is given for SDM model by (27) and DDM model by (28).

$$f_{SDM}(V, I, v) = I_{ph} - I_{o1}\left(e^{\frac{V+IR_s}{n_1 V_T}} - 1\right) - \frac{V + IR_s}{R_{sh}} - I \tag{27}$$

$$f_{SDM}\ (V, I, v) = I_{ph} - I_{01}\left(e^{\frac{V+IR_s}{n_1 V_T}} - 1\right) - I_{o2}\left(e^{\frac{V+IR_s}{n_2 V_T}} - 1\right) - \frac{V + IR_s}{R_{sh}} - I \tag{28}$$

The parameters can vary inside the chosen intervals during the algorithm running. These intervals are presented in Table 1 and are valid for all datasets used.

The number of search agents (population) and iterations were chosen after some trials, where the number of population and iterations varied. The best results are obtained for 250 search agents and 1500 iterations. These numbers are used for all applications of the two algorithms.

A. MJSC AT 41.5° C

The dataset was measured for MJSC at 41.5°C temperature, the current was calculated for the SDM and the DDM models, these values and errors are presented in Table S1 in the case of the BWOA algorithm and Table S2 for the CSA algorithm, respectively.

The values for the five or seven parameters obtained with BWOA and CSA algorithms, and 5P method are presented in Table 2, and the values for the four statistical tests are in Table 3 for both models and 5P method. Also, the computational time is presented. The algorithms and method run on the computer with the following specifications Intel Core i9, 3.6 GHz 20 MB; GPU: NVIDIA GeForce RTX 3080Ti 12 GB; RAM: 32 GB.

The best results are obtained when the BWOA algorithm is used. Variations exist between the extracted parameters using the BWOA and CSA algorithms for both models used. In the case of the SDM model, the I_{ph} differs with 0.12%, I_{o1} with 238%, n_1 with 6.6%, R_s with 11.1%, and R_{sh} with 34%, and the same behavior is found for the DDM model, except for two parameters that are specific to the generation recombination mechanism. The 5P methods give the highest value for the shunt resistance and the lowest reverse saturation current. So, the highest difference is between the reverse saturation currents and the shunt resistance. The stable parameter is the photogenerated current.

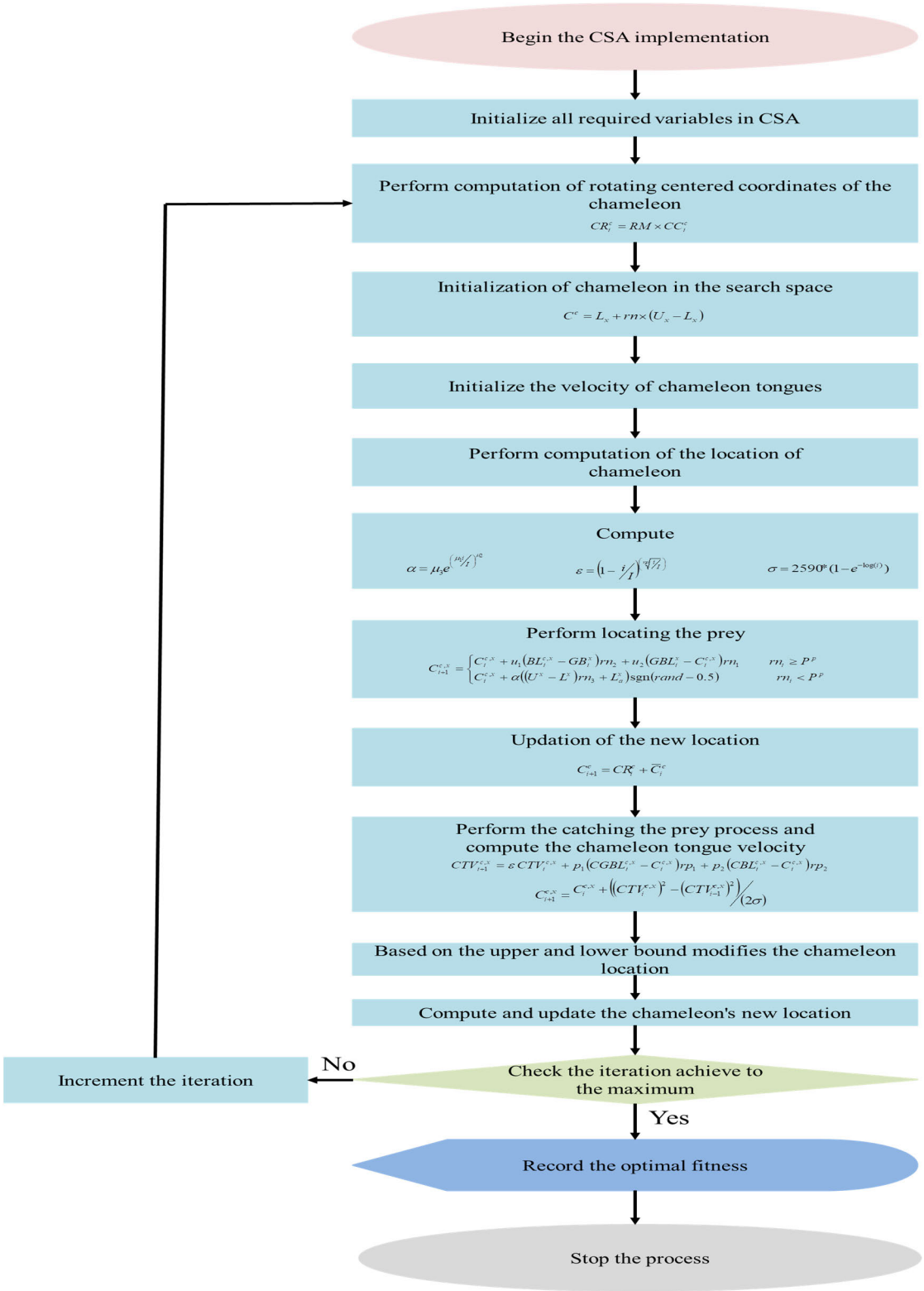

FIGURE 3. Workflow and procedure process of CSA.

The BWOA algorithm has the best performance in the extraction of the parameters in both the SDM and DDM models. The improvement in RMSE for the SDM model is 14.3%, and for the DDM model, it is 13.1%, compared with the CSA algorithm, and 4.28 times, compared with the 5P method. The same behavior is observed for the MAE and R^2.

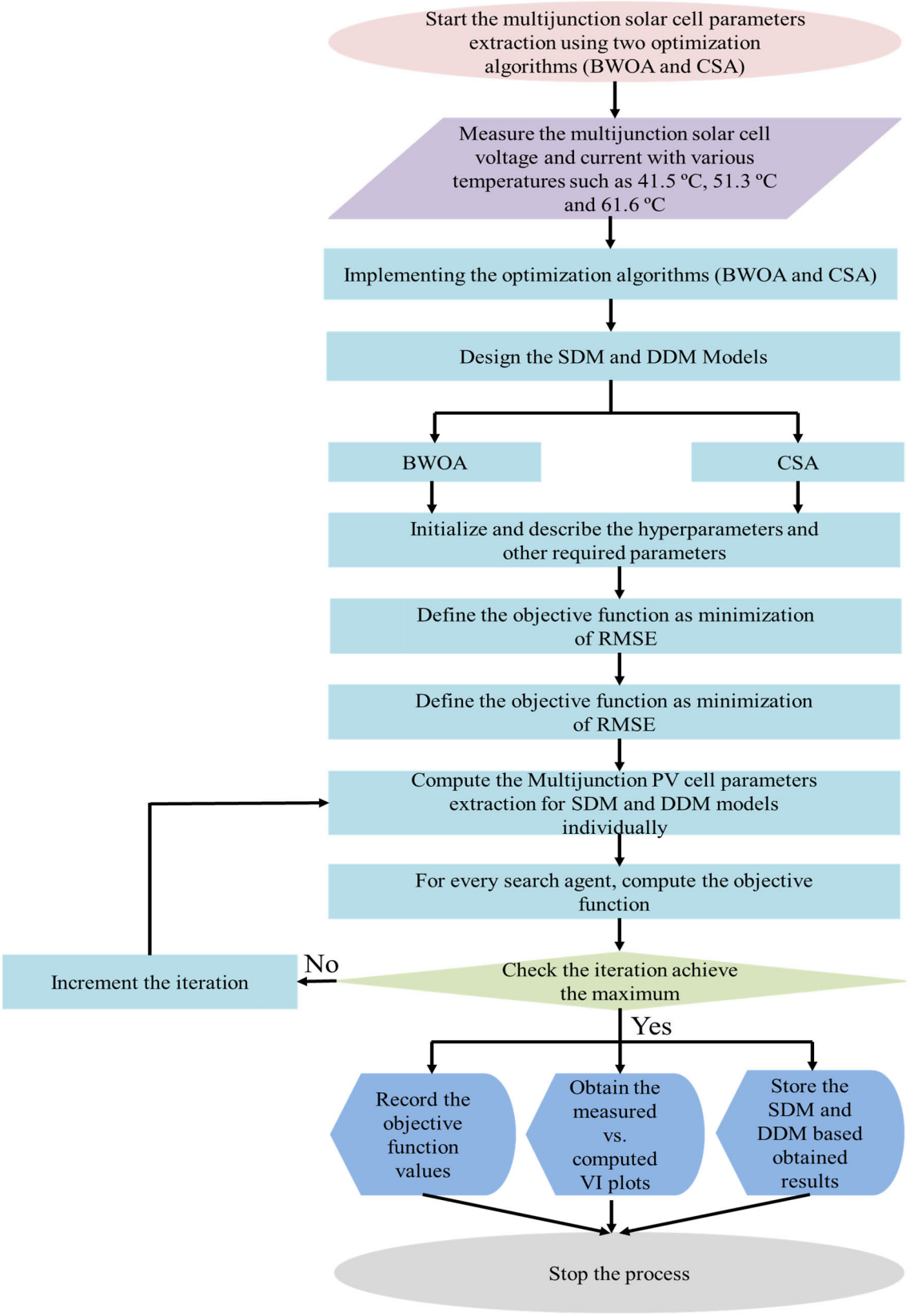

FIGURE 4. Generalized workflow of the multijunction PV cell parameter extraction.

TABLE 2. Parameters of the MJSC at 41.5°C.

Models	Algorithms	I_{ph} [A]	I_{o1} [A]	n_1	R_s [Ω]	R_{sh} [Ω]	I_{o2} [A]	n_2
SDM	BWOA	0.0121089428	2.3858024E-38	1.131912325	2.066927686	1.80398683206E+04	-	-
	CSA	0.0121243618	1.0000000E-40	1.06130028	2.296559350	1.34488398813E+04	-	-
	5P	0.01207129	1.671098E-35	1.230082	2.541460	22.30386E+04	-	-
DDM	BWOA	0.0121078162	2.3606317E-38	1.131921480	2.062849604	1.86903364737E+04	2.8573381684E-40	1.1319214800337
	CSA	0.0121315693	1.00000000E-40	1.061329620	2.293901938	1.40591135828E+04	1.4088443992E-22	2.2961082511610

TABLE 3. Statistical tests for MJSC at 41.5°C.

Models	Algorithms	RMSE	MAE	R^2	t-stat	Computational time [s]
SDM	**BWOA**	**8.9120260701E-5**	**6.56056E-5**	**0.99950163**	**0.0175632**	**2.021921**
	CSA	1.0186359636E-4	7.78534E-5	0.99934891	0.0235426	1.882829
	5P	3.8193717771E-4	3.80328E-3	0.99810284	3.2716	0
DDM	**BWOA**	**8.9123932518E-5**	**6.52022E-5**	**0.99950159**	**0.0763008**	**2.352401**
	CSA	1.0088314434E-4	7.59997E-5	0.99936139	0.139294	2.375248

The performance of the BWOA algorithm is proven by the smallest values of the t-stat, which is 25% smaller than that of the CSA algorithm for the SDM model and 45% for the DDM model respectively. This shows the overperformance of the BWOA algorithm for both models in comparison with the CSA algorithm.

The computational time is short, around 2 seconds. It is slightly higher for the BWOA algorithm than for the CSA algorithm in the case of the SDM model, and almost equal for the two algorithms in the case of DDM model. The computational time for the 5P method is very low, and it can be considered 0.

The measured current-voltage characteristics (blue) calculated using the BWOA algorithm (green), and with the CSA algorithm (red) are presented in Fig. 5a for the SDM model and Fig. 5b for the DDM model.

The two characteristics calculated using the BWOA and CSA algorithms match very well with the measured one for both models, SDM and DDM. The coefficient of determination for BWOA exceeds 0.9995 for both models, demonstrating the matching between the measured and calculated points.

The absolute current errors (ACE) are calculated for each pair's current-voltage (V,I) and plotted for both algorithms and models. See Fig. 6a for SDM and Fig.6b for the DDM model. BWOA algorithm has lower ACE values for all pairs in the case of the SDM model and almost the same for the DDM model, except for four pairs without significance.

B. MJSC AT 51.3° C

Tables S3 and S4 show the dataset measured for MJSC at 51.3°C temperature, the current calculated, and the errors for both models, SDM and DDM, in the case of the BWOA algorithm and the CSA algorithm, respectively.

The values for the five or seven parameters obtained with BWOA and CSA algorithms, and 5P method are presented in Table 4 and the values for the three statistical tests are in Table 5. Also, the computational time is presented.

The variations between the extracted parameters using the BWOA algorithm and the CSA algorithm for the SDM model are: the I_{ph} differs by 0.23%, for I_{o1} is more than 800 times, n_1 with 11.5%, R_s with 17.5% and R_{sh} with 60%. These are higher than in the case of 41.5°C temperature. In the case of the DDM model, a very small difference is observed for Io1, R_s, n_1 and I_{ph}, but high for R_{sh} and very high for I_{o2}. The difference for n_2 is 265%. The 5P method overestimates the values for almost all parameters I_o, R_s, R_{sh} and n.

BWOA algorithm has the best performance in the extraction of the parameters in the case of the SDM model, while the CSA is the best in the case of DDM model. The improvement in RMSE for SDM models is 7.7%, and for the DDM model is 9.5%. The method of 5P has the highest values for RMSE and MAE. The same behavior is observed for the next two statistical tests. The performance of the BWOA algorithm is proven by the smallest values of the t-stat, which is 39% smaller than that of the CSA algorithm for the SDM model and t-stat of DDM model in the case of CSA algorithm is very high. This shows the overperformance of the BWOA algorithm for both models in comparison with the CSA algorithm.

The computational time is small, around 2 s. The computational time for the 5P method is the lowest, almost 0. It is slightly higher for the BWOA algorithm than for the CSA algorithm, in the case of the SDM model, and almost equal for

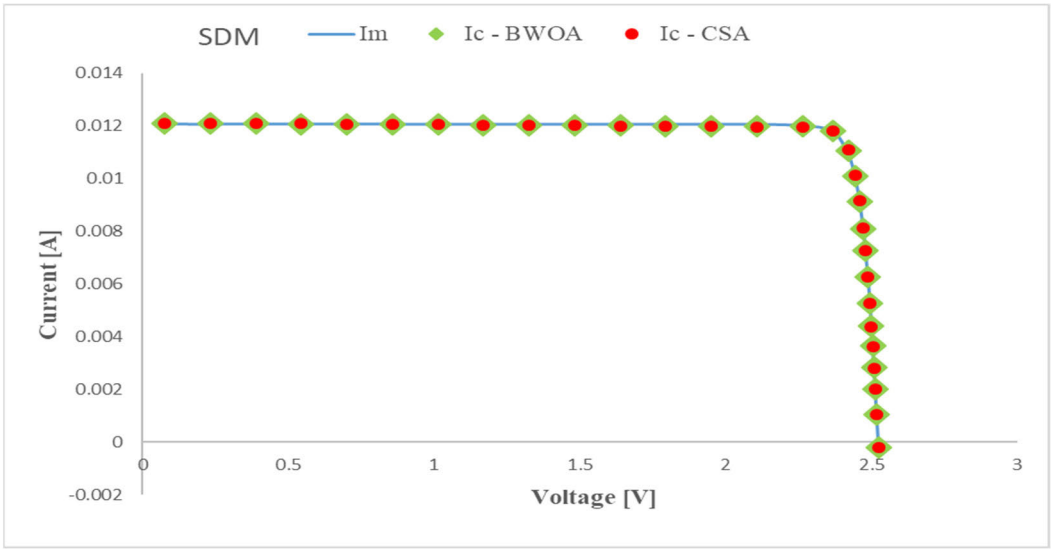

(a)

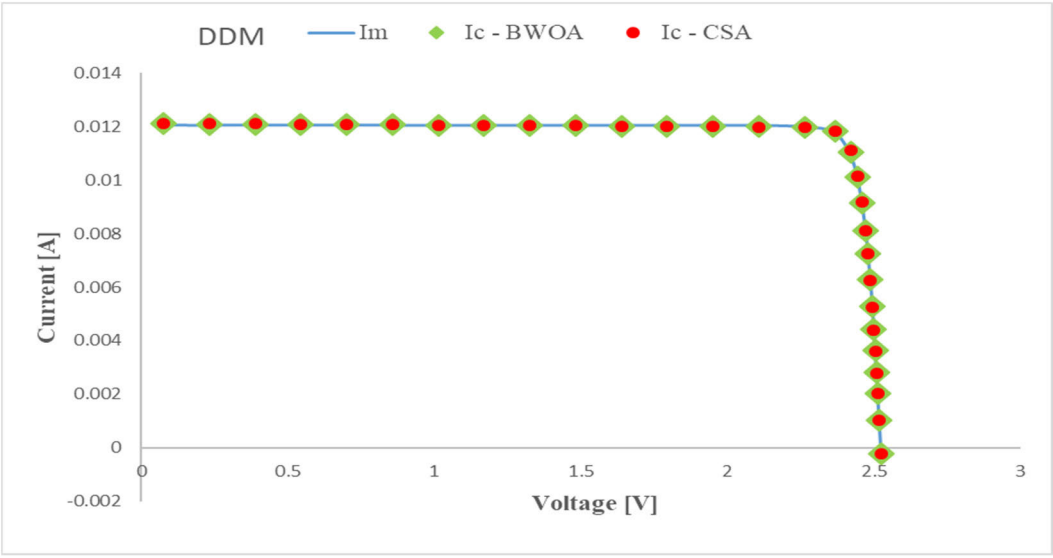

b)

FIGURE 5. Current-voltage characteristics were measured and calculated using BWOA and CSA algorithms at 41.5°C temperature: a) for the SDM model; b) for the DDM model.

TABLE 4. Parameters of the MJSC at 51.3°C.

Models	Algorithms	I_{ph} [A]	I_{o1} [A]	n_1	R_s [Ω]	R_{sh} [Ω]	I_{o2} [A]	n_2
SDM	BWOA	0.012382443	8.6249412E-37	1.116353946	2.126612851	1.59487273133E+04	-	-
	CSA	0.012411336	1.0000000E-40	1.001110303	2.499590378	9.95465622131E+03	-	-
	5P	0.01235383	6.068981E-36	1.144978	2.655795	2.301152E+04	-	-
DDM	BWOA	0.012293709	2 1.0091098E-40	1.009109865	2.528407915	1E+05	1.0091098655E-40	1.1319214800337
	CSA	0.012442539	1 1.00000000E-40	1.001164676	2.462677040	9.76066361006E+03	2.6221828882E-17	2.9999999990733

the two algorithms in the case of DDM model. CSA algorithm presents a very small increase for the last model.

The measured current-voltage characteristics (blue) calculated using the BWOA algorithm (green), and with the CSA

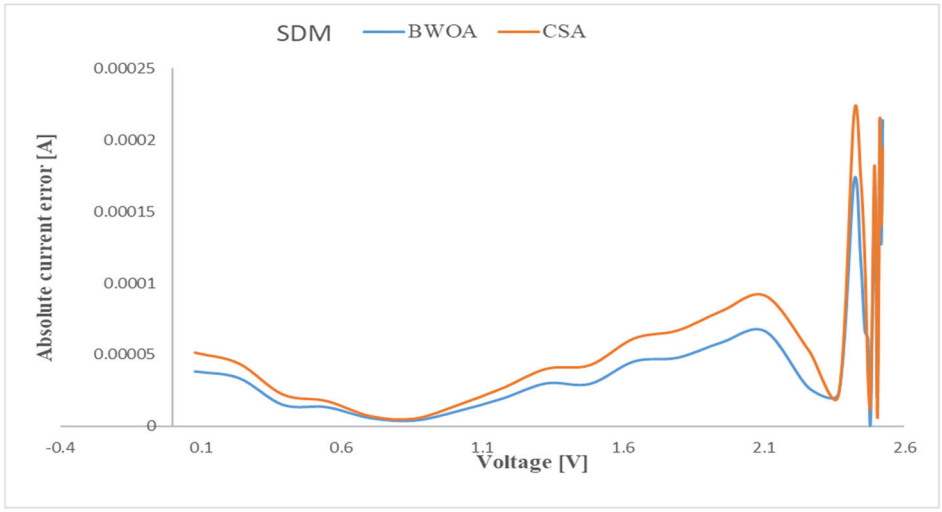

(a)

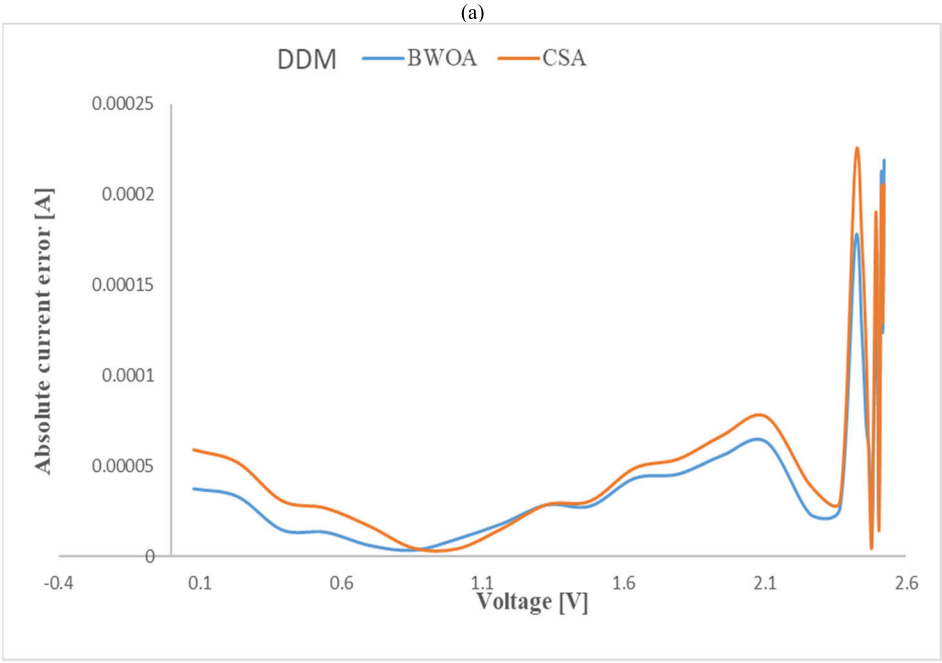

b)

FIGURE 6. Absolute current errors were calculated using BWOA and CSA algorithms: a) for the SDM model; b) for the DDM model.

TABLE 5. Statistical tests for MJSC at 51.3°C.

Models	Algorithms	RMSE	MAE	R^2	t-stat	Computational time [s]
SDM	**BWOA**	**9.4508986452E-5**	**7.54796E-5**	**0.9994632**	**0.0438425**	**2.112030**
	CSA	1.0186359636E-4	1.00411E-4	0.9990913	0.070477	1.997282
	5P	3.2891868735E-4	1.98625E-4	0.9934984	3.45664	0
DDM	BWOA	1.3016613407E-4	1.0121E-4	0.9989817	0.00104256	2.267707
	CSA	**1.1884566045E-4**	**9.81952E-5**	**0.9991511**	**0.353326**	**2.277469**

algorithm (red) are presented in Fig. 7a for the SDM model and Fig. 7b for the DDM model.

The two characteristics calculated using the BWOA and CSA algorithms perfectly match the measured ones for both

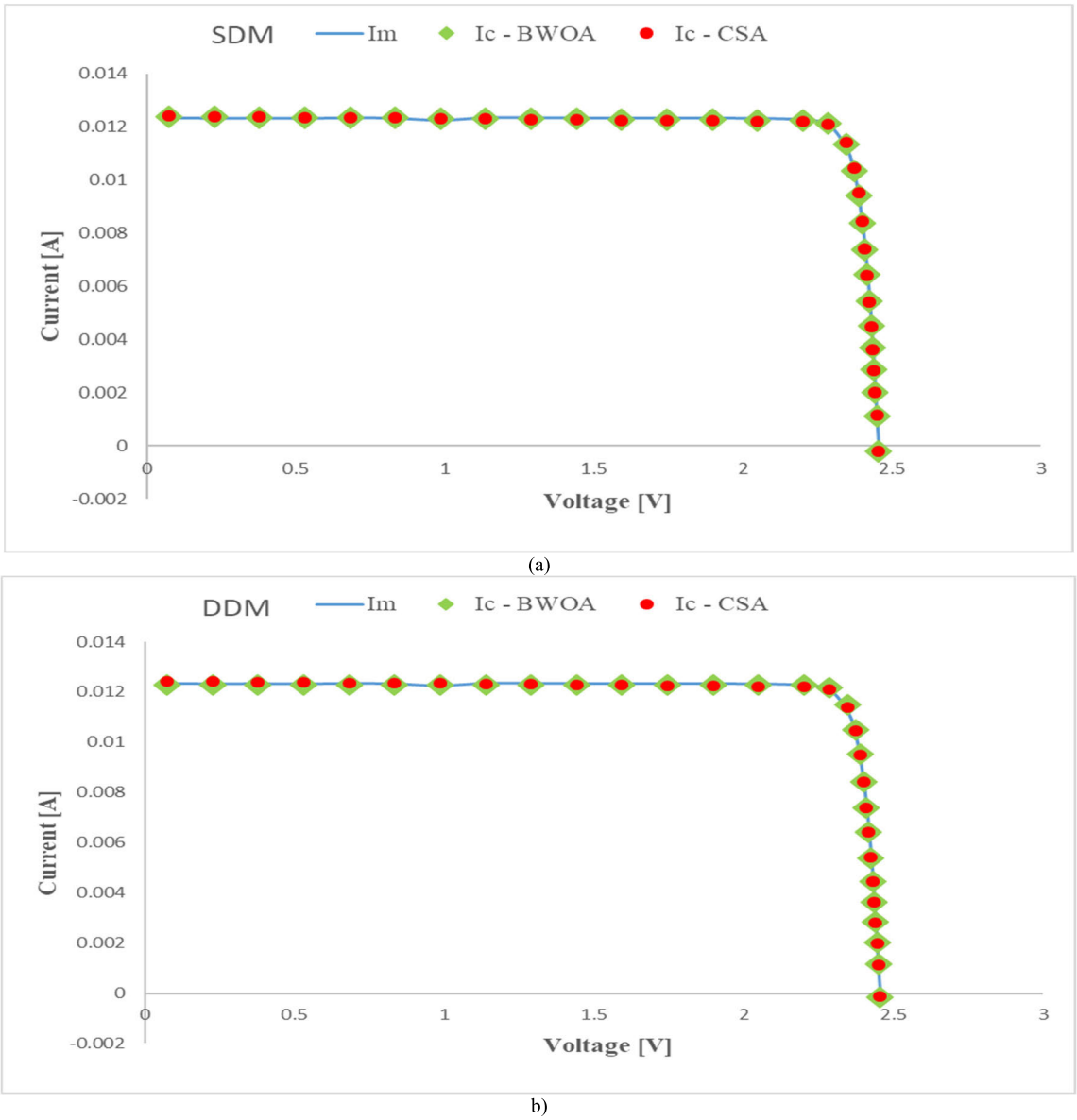

FIGURE 7. Current-Voltage characteristics were measured and calculated using BWOA and CSA algorithms at 51.3°C temperature: a) for the SDM model; b) for the DDM model.

models, SDM and DDM, in accordance with the results of the applied statistical tests.

The coefficient of determination for BWOA exceeds 0.9994 for SDM model and almost 0.999 for DDM model, demonstrating the matching between the measured and calculated points. These values are slightly smaller than those for the datasets at 41.5°C. It can be observed that the calculated pairs with the CSA algorithm have minimal matching problems around the short circuit current.

The absolute current errors (ACE) are calculated for each pair's current-voltage (V, I) and plotted for both algorithms and models. See Fig. 8a for SDM and Fig. 8b for the DDM model. BWOA algorithm has lower ACE for almost all pairs, except for three pairs around the voltage 1V, in the case of the SDM model. In the case of the DDM model, there is an oscillation between two ACEs for BWOA and CSA algorithms.

C. MJSC AT 61.6°C

Tables S5 and S6 show the dataset measured for MJSC at 61.6°C temperature, the current calculated and the errors for the SDM model in the case of both algorithms BWOA and CSA. In the case of the DDM model, the results are inconclusive, and they are not considered, perhaps due to excess measurement noise [16]. The CSA algorithm encountered the same problems in extracting the parameters, even the SDM model, see Fig. 9.

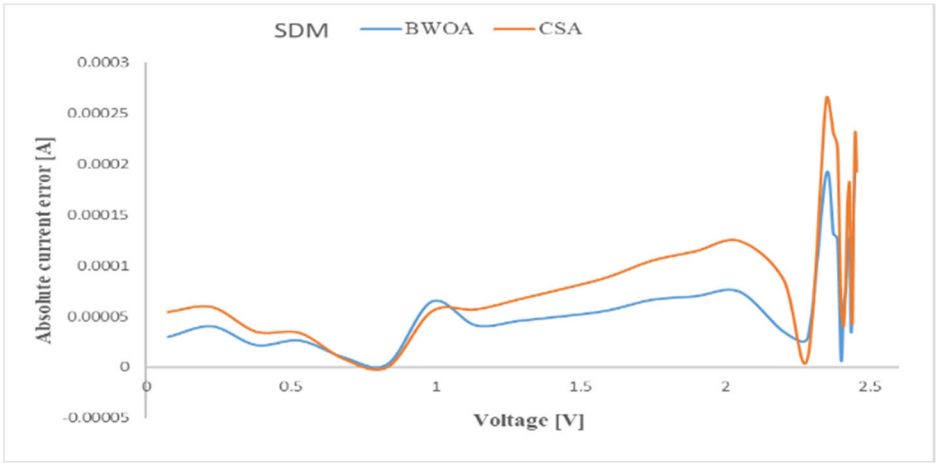

(a)

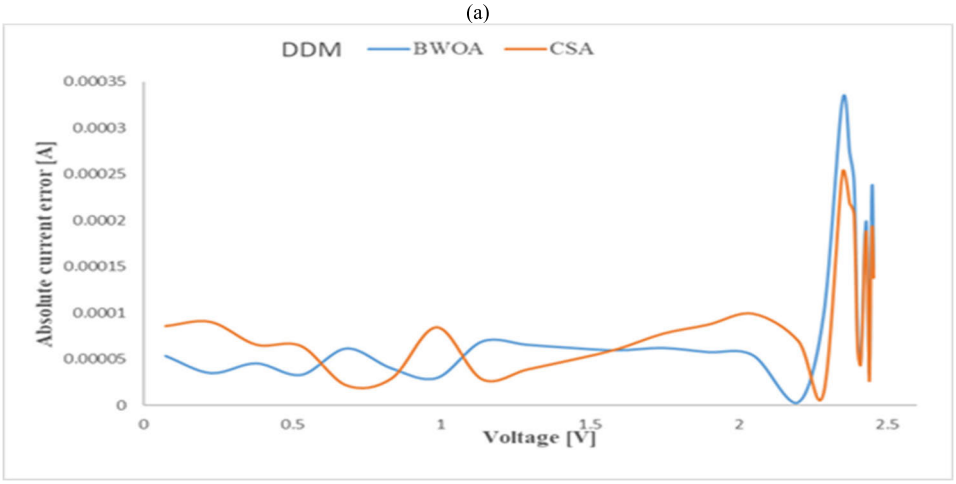

b)

FIGURE 8. Absolute current errors were calculated using BWOA and CSA algorithms: a) for the SDM model; b) for the DDM model.

TABLE 6. Parameters of the MJSC at 61.6°C.

Models	Algorithms	I_{ph} [A]	I_{o1} [A]	n_1	R_s [Ω]	R_{sh} [Ω]
SDM	BWOA	0.0126463735	1.7564737E-35	1.09267609	2.173965484	1.07646947093E+04
	CSA	0.0126663735	1.8464737E-35	1.0950162684	2.16696549	1.07807048E+04
	5P	0.01258102	1.858120E-30	1.290024	2.212063	6.414171E+04

The values for the five parameters obtained with BWOA and CSA algorithms, as well as for the 5P method, are presented in Table 6, and the values for the three statistical tests are in Table 7. Also, the computational time is presented. The extracted parameters by the CSA algorithm are overestimated as I_{ph}, I_{o1}, and n_1 or underestimated as R_s and R_{sh}.

RMSE obtained using the BWOA algorithm is six times lower than the one obtained with CSA and 3.3 with 5P, respectively. Also, MAE has the same behaviour, and the coefficient of determination for the CSA algorithm is low compared to the current voltage characteristic calculated with the CSA algorithm. It can be observed for the first part of the current-voltage characteristic until its knee that the current is overestimated, Fig. 9.

The performance of the BWOA algorithm is proven by the smallest values of the t-stat, which are very low in comparison with that of the CSA algorithm for the SDM. This shows the overperformance of the BWOA algorithm for the SDM model in comparison with the CSA algorithm.

The computational time is short, around 2 seconds. It is slightly higher for the BWOA algorithm than for the CSA algorithm in the case of the SDM model.

The two characteristics calculated using the BWOA and CSA algorithms match very well with the measured one for SDM model. The coefficient of determination for BWOA

TABLE 7. Statistical tests for MJSC at 61.6°C.

Models	Algorithms	RMSE	MAE	R^2	t-stat	Computational time [s]
	BWOA	**9.6816850966E-5**	**7.51217E-5**	**0.9994666**	**0.0391282**	**1.993307**
SDM	CSA	5.6947272673E-4	3.74804E-4	0.98154654	4.05785	1.975035
	5P	3.2115343257E-4	1.90824E-4	0.9941310	3.44578	0

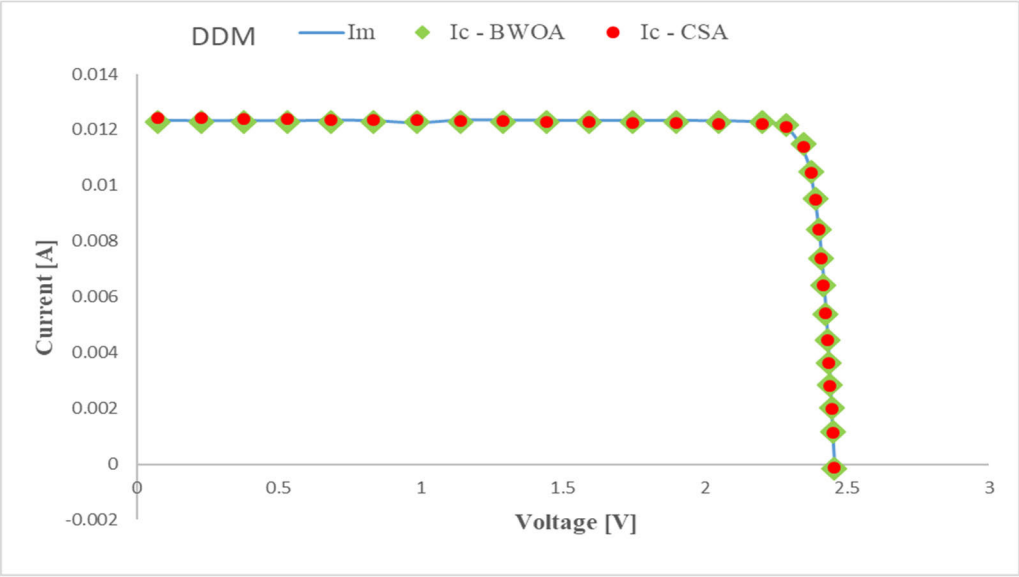

FIGURE 9. Current-Voltage characteristics were measured and calculated using BWOA and CSA algorithms at 61.6°C temperature for the SDM model.

exceeds 0.9994 for SDM model, while for CSA algorithm it is 0.982.

The absolute current errors (ACE) are calculated for each pair (V, I), for both algorithms and the SDM model, and are plotted in Fig. 10. CSA algorithm has higher ACE values for almost all pairs, which shows that it remains in a local minimum due to the measured noisy characteristic.

RMSE increases with the increase of the solar cell temperature, Fig.11. This increase can be due to the noise of the measured current-voltage characteristics. The increase is by 8.6% in the case of the 61.6°C temperature compared to 41.5°C.

The best results obtained to extract the parameters of the multijunction solar cell for three temperatures are obtained using the BWOA algorithm for the SDM model. This shows that, for the MJSC using the SDM model, it is enough, and the computing time is slightly lower.

Using metaheuristic algorithms provides very accurate parameters for the extraction of solar cells. In this study, the best solutions are obtained using the BWOA algorithm. Their behavior in terms of temperature can be analyzed using the extracted parameters. This dependence for the five parameters is presented in Fig. 12. Four of the five dependencies are linear. The reverse saturation current has an exponential dependence, Fig.12b. The photogenerated current increases with temperature growth, Fig.12a. The I_{ph} temperature coefficient is 3E-5A/°C. The series resistance increases linearly, Fig.12c. The shunt resistance, Fig.12d, and the ideality factor of the diode decrease, Fig.12e, linearly with temperature growth.

D. CTJ 30 AT 25°C

The two algorithms, BWOA and CSA, are applied to a dataset from research literature for comparison [42]. This dataset is for a multijunction panel with CTJ 30 solar cell [57].

Table S7 shows the dataset that measured the CTJ panel at 25° C temperature [42], and the current calculation uses the SDM model in the case of both algorithms BWOA and CSA.

The values for the five parameters obtained with BWOA, CSA algorithms, 5P method, and the method developed in [42], SM, are presented in Table 8, and the values for the three statistical tests are presented in Table 9.

There is a significant variation for the reverse saturation current from 1.14504835E-14 A for BWOA algorithm to 7.729626E-17 A for 5P method, for series resistance from 0.0746368274Ω for BWOA algorithm to 0.1227011Ω for 5P method and for shut resistance from 1.86963045E+3 Ω for BWOA algorithm to 506.3099 Ω for 5P method, respectively. The extracted parameters for CTJ 30 panel using BWOA and CSA are closer, but the reverse saturation current and the shunt resistance vary a lot. The same behavior is for the

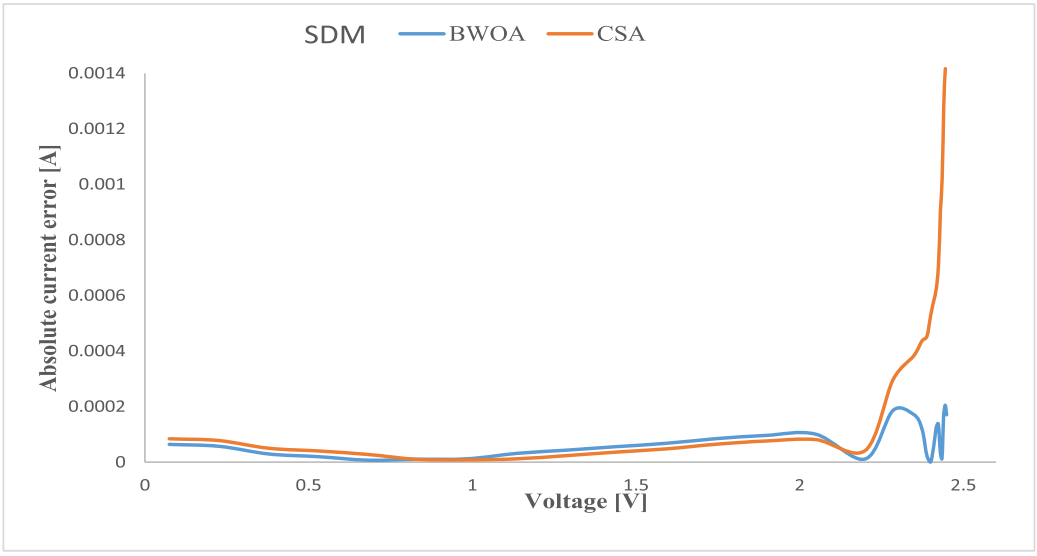

FIGURE 10. Current-voltage characteristics were measured and calculated using BWOA and CSA algorithms at 61.6°C temperature for the SDM model.

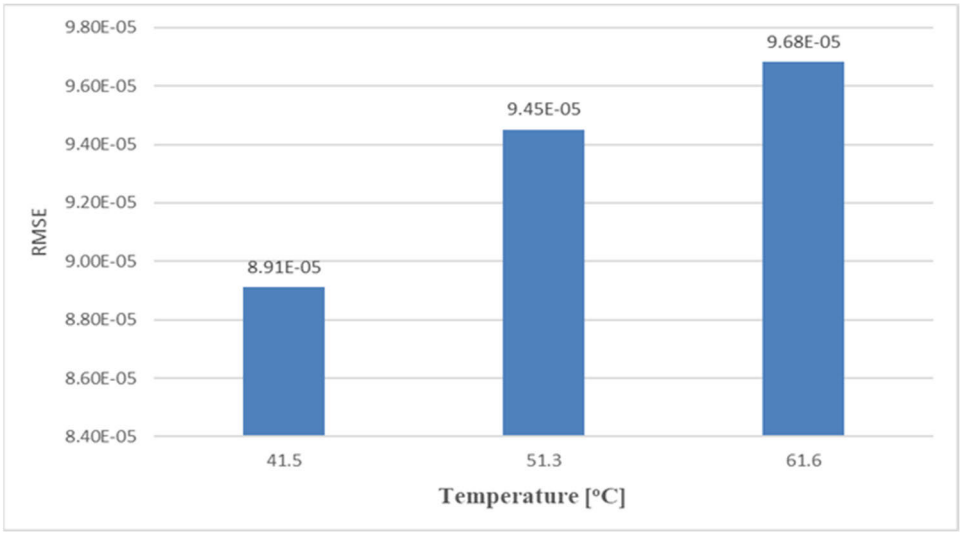

FIGURE 11. Current-voltage behavior RMSE for BWOA algorithm in the function of the temperature.

TABLE 8. Parameters of the CTJ 30 at 25°C.

Models	Algorithms	I_{ph} [A]	I_{o1} [A]	n_1	R_s [Ω]	R_{sh} [Ω]
SDM	BWOA	0.471041514	1.14504835E-14	3.24086801	0.0746368274	1.86963045E+3
	CSA	0.4702427851	7.21800719E-15	3.19413875	0.0793857084	3.33172673E+3
	SM	0.473	2.83E-15	3.1	0.055	425
	5P	0.4732580	7.729626E-17	2.795478	0.1227011	506.3099

parameters extracted using the SM method in comparison with the ones obtained by the BWOA algorithm.

RMSE obtained using the BWOA is the lowest in comparison with those calculated for the other three methods. The worst RMSE is obtained for the SM method. The same behavior is for the MAE and R^2 statistical tests. The performance of the BWOA algorithm is proven by the smallest values of the t-stat, which are very low in comparison with that of the SM and 5P methods for the SDM. The t-stat for BWOA is lower by almost 7% than the one given by the CSA

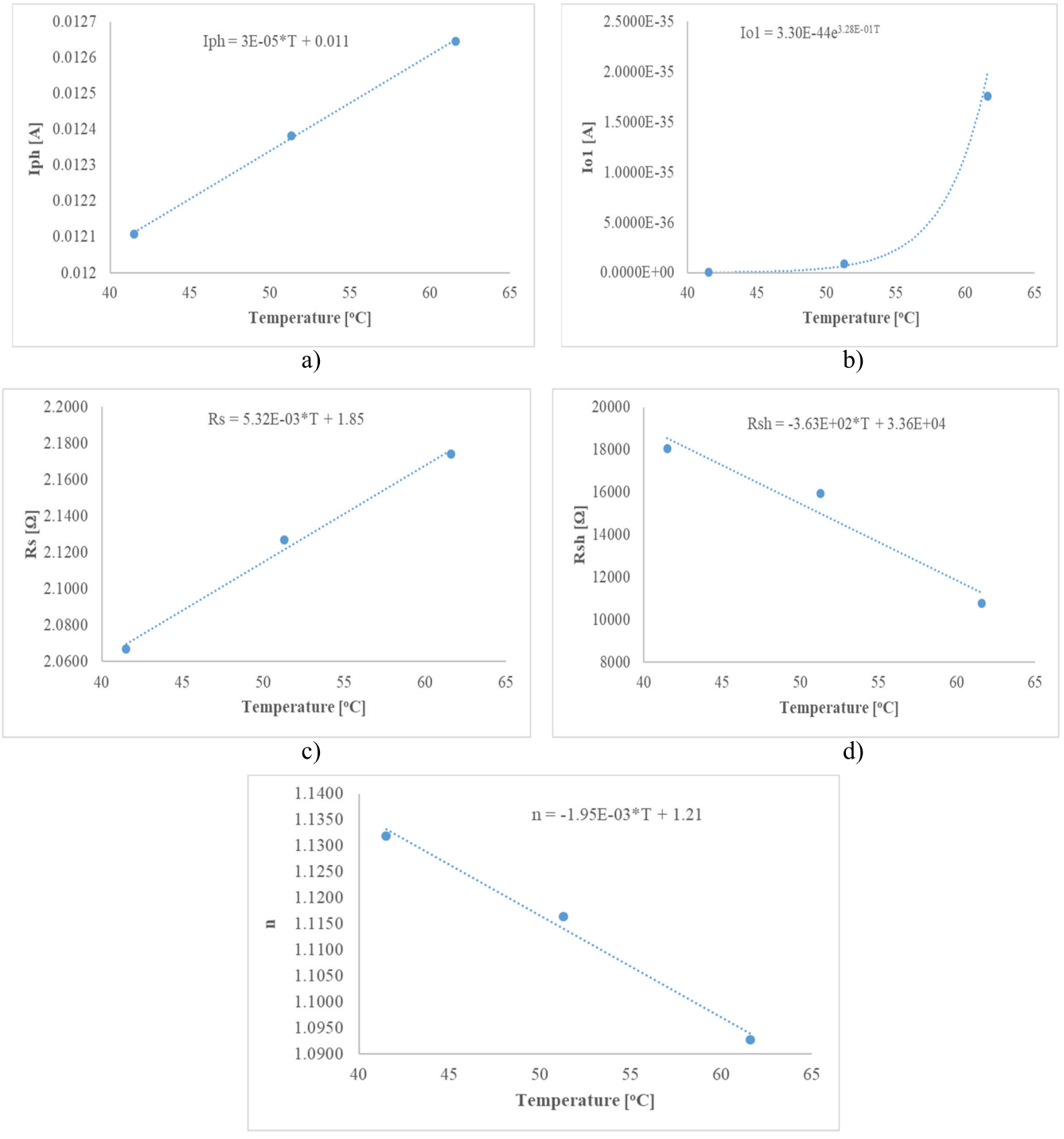

FIGURE 12. The five parameters of dependence vs temperature: a) I_{ph}; b) I_{o1}; c) R_s; d) R_{sh}; and e) n_1.

algorithm. The values obtained for the four statistical tests show the supremacy of the BWOA and CSA algorithms.

The measured current-voltage characteristics (blue), calculated using the BWOA algorithm (green), and with the CSA algorithm (red), are presented in Fig. 13 for the SDM.

The two characteristics calculated using the BWOA and CSA algorithms perfectly match the measured ones for the SDM model, in accordance with the results of the applied statistical tests. The coefficient of determination for BWOA and CSA exceeds 0.9994 for SDM model, while for SM is the lowest one, 0.9975.

TABLE 9. Statistical tests for CTJ 30 at 25°C.

Models	Algorithms	RMSE	MAE	R^2	t-stat	Computational time [s]
SDM	**BWOA**	**3.62E-3**	**2.51643E-3**	**0.9994100**	**0.0605843**	**1.9941**
	CSA	3.6250156794E-3	2.63709E-3	0.9994084	0.0656531	1.975035
	SM	7.3775783929E-3	4.54905E-3	0.9975498	1.7325	-
	5P	6.4918775917E-3	3.80328E-3	0.9981028	1.15811	0

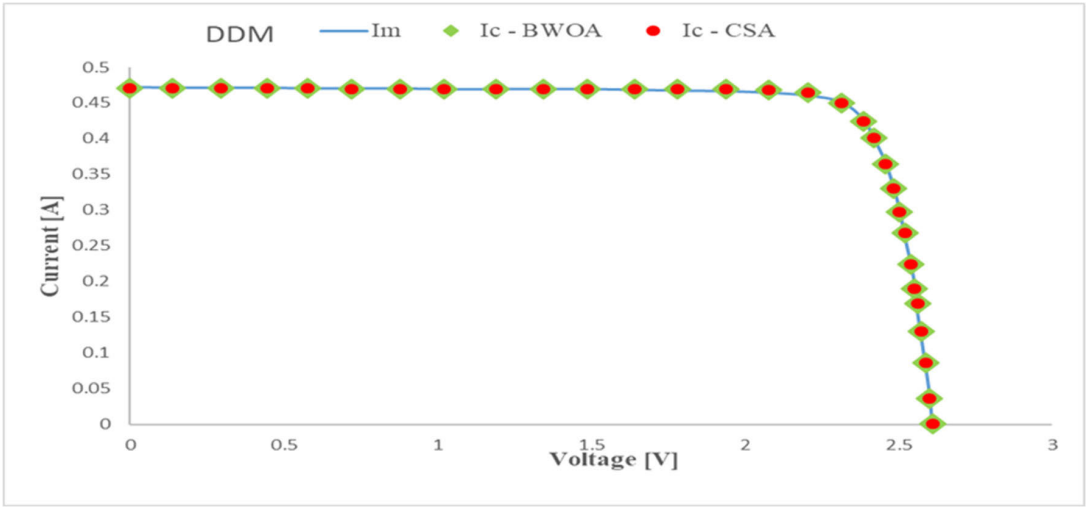

FIGURE 13. Current-voltage characteristics measured and calculated using BWOA and CSA algorithms at 25°C temperature in case of the SDM model.

FIGURE 14. Absolute current errors calculated using BWOA and CSA algorithms for the SDM model.

The absolute current errors (ACE) are calculated for each pair current-voltage (V, I) and for BWOA and CSA algorithms and are plotted for the SDM model, see Fig. 14. In this case, there is an oscillation between two ACEs for BWOA and CSA algorithms.

The comparison for time computing for BWOA and CSA algorithms in the case of the SDM model is shown in Fig.15.

The CSA algorithm has the lower time computing for all four cases considered in comparison with the one for BWOA. The variation of the difference in time consuming is from

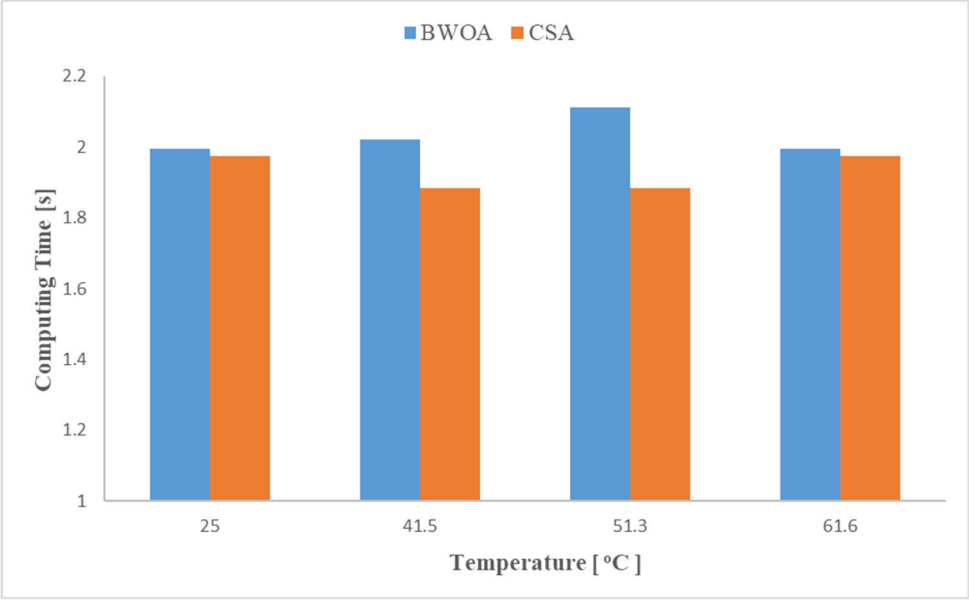

FIGURE 15. Time computing calculated for BWOA and CSA algorithms in case of the SDM model.

under 1% to 12%. In the case of 41.5°C for the solar cell and 25°C for the panel the computing time is practical equal. The highest difference is obtained for 51.3°C dataset and it is 12%.

IV. CONCLUSION

Two algorithms were applied to extract the parameters of the multijunction solar cell for two models, SDM and DDM, respectively. The Chameleon Swarm Algorithm is redesigned and implemented for the first time to extract the parameters of the multijunction solar cell. Also, the Black Widow Optimization Algorithm is applied for the first time to extract the parameters of the multijunction solar cell. Both algorithms are applied for two models, SDM and DDM.

Four statistical tests are considered to analyze the performance of the two algorithms applied to the three datasets. The main statistical test is RMSE.

A dataset from the research literature, for CTJ 30 panel, is considered to validate the performance of the two considered algorithms. The four statistical tests show that the BWOA is the best and the second best is the CSA algorithm. To validate the performance of the algorithms, the RMSE is compared with one from specialized literature. It varies from 3.62E-3 for BWOA, to 7.3775783929E-3 for the SM. The RMSE in the case of CSA is 3.6250156794E-3 close to the one obtained by the BWOA algorithm. The t-stat used to prove the performance of the algorithms shows that the BWOA algorithm is the best.

The BWOA algorithm gives the best results for all cases studied, except for the DDM model, which is applied for current-voltage characteristics measured at 51.3°C. All three values for RMSE calculated with the BWOA algorithm are lower in the case of SDM than those for the DDM model. This shows that using the SDM model is enough for the MJSC.

The computing time is also calculated for each case considered. It is around 2s for all cases studied. Comparatively, in the case of the BWOA algorithm, it is higher for the DDM model by 7.4% and 16.3% than for the SDM model. CSA has the lowest computing time for all four cases considered, varying from 1.882829 s to 2.277469 s. The highest difference for time computing between the CSA and BWOA is obtained for 51.3°C and it is around 12%. Short time computing is a big advantage for PV manufacturers because it leads to increased work productivity.

Using the accurately extracted parameters of the multijunction solar cell, the dependences in the function of the temperature are obtained. For four of the parameters, these dependences are linear, two of them with positive slope, for I_{ph} and R_s, and for the other two with a negative slope, n_1 and R_{sh}. The fifth, I_{o1}, dependence is exponential. Reducing complexity, processing time, and optimizing results are the ultimate benefits of this research endeavour: extracting precise multijunction solar cells.

Limitations of the proposed algorithm are iterative in nature.

In future works, the dependence between the five parameters of the multijunction solar cell and the irradiance for concentrated light will be analyzed. The temperature will also be considered. The computation time-based analysis will be performed for various PC configurations. The parameters will be extracted using both algorithms presented in this paper. Also, the extraction of the parameters for each subcell of the multijunction solar cell will be achieved using the equivalent circuit with three SDM models connected in series by both BWOA and CSA algorithms.

REFERENCES

[1] REN2021. (2022). *Renewables 2022 Global Status Report*. Accessed: Jan. 20, 2024. [Online]. Available: https://www.ren21.net/wp-content/uploads/2019/05/GSR2022_Full_Report.pdf

[2] D. Gielen, F. Boshell, D. Saygin, M. D. Bazilian, N. Wagner, and R. Gorini, "The role of renewable energy in the global energy transformation," *Energy Strategy Rev.*, vol. 24, pp. 38–50, Apr. 2019, doi: 10.1016/j.esr.2019.01.006.

[3] F. J. Gómez-Gil, X. Wang, and A. Barnett, "Analysis and prediction of energy production in concentrating photovoltaic (CPV) installations," *Energies*, vol. 5, no. 3, pp. 770–789, Mar. 2012, doi: 10.3390/en5030770.

[4] S. P. Philipps, A. W. Bett, K. Horowitz, and S. Kurtz, "Current status of concentrator photovoltaic (CPV) technology," Fraunhofer ISE/NREL, Rep. TP-5J00-65130, 2015, doi: 10.2172/1351597.

[5] A. M. Soomar, A. Hakeem, M. Messaoudi, P. Musznicki, A. Iqbal, and S. Czapp, "Solar photovoltaic energy optimization and challenges," *Frontiers Energy Res.*, vol. 10, pp. 1–18, May 2022, doi: 10.3389/fenrg.2022.879985.

[6] M. Steiner, G. Siefer, T. Hornung, G. Peharz, and A. W. Bett, "YieldOpt, a model to predict the power output and energy yield for concentrating photovoltaic modules," *Prog. Photovoltaics, Res. Appl.*, vol. 23, no. 3, pp. 385–397, Mar. 2015, doi: 10.1002/pip.2458.

[7] R. M. France, J. F. Geisz, T. Song, W. Olavarria, M. Young, A. Kibbler, and M. A. Steiner, "Triple-junction solar cells with 39.5% terrestrial and 34.2% space efficiency enabled by thick quantum well superlattices," *Joule*, vol. 6, no. 5, pp. 1121–1135, May 2022, doi: 10.1016/j.joule.2022.04.024.

[8] J. F. Geisz, R. M. France, K. L. Schulte, M. A. Steiner, A. G. Norman, H. L. Guthrey, M. R. Young, T. Song, and T. Moriarty, "Six-junction III-V solar cells with 47.1% conversion efficiency under 143 suns concentration," *Nature Energy*, vol. 5, no. 4, pp. 326–335, Apr. 2020, doi: 10.1038/s41560-020-0598-5.

[9] X. Chen, F. Xu, and K. He, "Multi-region combined heat and power economic dispatch based on modified group teaching optimization algorithm," *Int. J. Electr. Power Energy Syst.*, vol. 155, Jan. 2024, Art. no. 109586, doi: 10.1016/j.ijepes.2023.109586.

[10] X. Chen, S. Fang, and K. Li, "Reinforcement-learning-based multi-objective differential evolution algorithm for large-scale combined heat and power economic emission dispatch," *Energies*, vol. 16, no. 9, p. 3753, Apr. 2023, doi: 10.3390/en16093753.

[11] A. M. Deaconu, D. T. Cotfas, and P. A. Cotfas, "Calculation of seven photovoltaic cells parameters using parallelized successive discretization algorithm," *Int. J. Photoenergy*, vol. 2020, pp. 1–13, Dec. 2020, doi: 10.1155/2020/6669579.

[12] B. R. Uma, S. Krishnan, V. Radhakrishna, and R. Campesato, "Effect of space radiation on CTJ new version multijunction solar cells," *Radiat. Effects Defects Solids*, vol. 176, nos. 3–4, pp. 382–395, Mar. 2021, doi: 10.1080/10420150.2020.1849214.

[13] E. F. Fernández, J. P. Ferrer-Rodríguez, F. Almonacid, and P. Pérez-Higueras, "Current-voltage dynamics of multi-junction CPV modules under different irradiance levels," *Sol. Energy*, vol. 155, pp. 39–50, Oct. 2017, doi: 10.1016/j.solener.2017.06.012.

[14] E. F. Fernández, P. Pérez-Higueras, F. Almonacid, J. A. Ruiz-Arias, P. Rodrigo, J. I. Fernandez, and I. Luque-Heredia, "Model for estimating the energy yield of a high concentrator photovoltaic system," *Energy*, vol. 87, pp. 77–85, Jul. 2015, doi: 10.1016/j.energy.2015.04.095.

[15] A. Ben Or and J. Appelbaum, "Estimation of multi-junction solar cell parameters," *Prog. Photovoltaics, Res. Appl.*, vol. 21, no. 4, pp. 713–723, Jun. 2013, doi: 10.1002/pip.2158.

[16] A. Mohapatra, B. Nayak, P. Das, and K. B. Mohanty, "A review on MPPT techniques of PV system under partial shading condition," *Renew. Sustain. Energy Rev.*, vol. 80, pp. 854–867, Dec. 2017, doi: 10.1016/j.rser.2017.05.083.

[17] N. Rawat, P. Thakur, A. K. Singh, and R. C. Bansal, "Performance analysis of solar PV parameter estimation techniques," *Optik*, vol. 279, May 2023, Art. no. 170785, doi: 10.1016/j.ijleo.2023.170785.

[18] H. M. Ridha, H. Hizam, S. Mirjalili, M. L. Othman, M. E. Ya'acob, and L. Abualigah, "A novel theoretical and practical methodology for extracting the parameters of the single and double diode photovoltaic models," *IEEE Access*, vol. 10, pp. 11110–11137, 2022, doi: 10.1109/ACCESS.2022.3142779.

[19] R. Venkateswari and N. Rajasekar, "Review on parameter estimation techniques of solar photovoltaic systems," *Int. Trans. Electr. Energy Syst.*, vol. 31, no. 11, Nov. 2021, Art. no. 131132021, doi: 10.1002/2050-7038.13113.

[20] D. T. Cotfas, P. A. Cotfas, and S. Kaplanis, "Methods to determine the DC parameters of solar cells: A critical review," *Renew. Sustain. Energy Rev.*, vol. 28, pp. 588–596, Dec. 2013, doi: 10.1016/j.rser.2013.08.017.

[21] A. M. Humada, M. Hojabri, S. Mekhilef, and H. M. Hamada, "Solar cell parameters extraction based on single and double-diode models: A review," *Renew. Sustain. Energy Rev.*, vol. 56, pp. 494–509, Apr. 2016, doi: 10.1016/j.rser.2015.11.051.

[22] S. Li, W. Gong, and Q. Gu, "A comprehensive survey on meta-heuristic algorithms for parameter extraction of photovoltaic models," *Renew. Sustain. Energy Rev.*, vol. 141, May 2021, Art. no. 110828, doi: 10.1016/j.rser.2021.110828.

[23] B. Yang, J. Wang, X. Zhang, T. Yu, W. Yao, H. Shu, F. Zeng, and L. Sun, "Comprehensive overview of meta-heuristic algorithm applications on PV cell parameter identification," *Energy Convers. Manage.*, vol. 208, Mar. 2020, Art. no. 112595, doi: 10.1016/j.enconman.2020.112595.

[24] M. A. Navarro, D. Oliva, A. Ramos-Michel, and E. H. Haro, "An analysis on the performance of metaheuristic algorithms for the estimation of parameters in solar cell models," *Energy Convers. Manag.*, vol. 276, Jan. 2023, Art. no. 116523, doi: 10.1016/j.enconman.2022.116523.

[25] X. Chen, S. Wang, and K. He, "Parameter estimation of various PV cells and modules using an improved simultaneous heat transfer search algorithm," *J. Comput. Electron.*, vol. 23, no. 3, pp. 584–599, Jun. 2024, doi: 10.1007/s10825-024-02153-w.

[26] R. Abbassi, S. Saidi, S. Urooj, B. N. Alhasnawi, M. A. Alawad, and M. Premkumar, "An accurate metaheuristic mountain gazelle optimizer for parameter estimation of single- and double-diode photovoltaic cell models," *Mathematics*, vol. 11, no. 22, p. 4565, 2023, doi: 10.3390/math11224565.

[27] P. A. Kumari, C. H. H. Basha, F. Fathima, C. Dhanamjayulu, H. Kotb, and A. Elrashidi, "Adaptive RAO ensembled dichotomy technique for the accurate parameters extraction of solar PV system," *Sci. Rep.*, vol. 14, no. 1, p. 2920, 2024, doi: 10.1038/s41598-024-63383-3.

[28] R. Abbassi, A. Abbassi, A. A. Heidari, and S. Mirjalili, "An efficient salp swarm-inspired algorithm for parameters identification of photovoltaic cell models," *Energy Convers. Manage.*, vol. 179, pp. 362–372, Jan. 2019, doi: 10.1016/j.enconman.2018.10.069.

[29] H. A. Ramadan, B. Khan, and A. A. Z. Diab, "Accurate parameters estimation of three diode model of photovoltaic modules using hunter–prey and wild horse optimizers," *IEEE Access*, vol. 10, pp. 87435–87453, 2022, doi: 10.1109/ACCESS.2022.3199001.

[30] D. T. Cotfas, A. M. Deaconu, and P. A. Cotfas, "Hybrid successive discretization algorithm used to calculate parameters of the photovoltaic cells and panels for existing datasets," *IET Renew. Power Generat.*, vol. 15, no. 15, pp. 3661–3687, Nov. 2021, doi: 10.1049/rpg2.12262.

[31] A. Abbassi, R. Abbassi, A. A. Heidari, D. Oliva, H. Chen, A. Habib, M. Jemli, and M. Wang, "Parameters identification of photovoltaic cell models using enhanced exploratory salp chains-based approach," *Energy*, vol. 198, May 2020, Art. no. 117333, doi: 10.1016/j.energy.2020.117333.

[32] J. Montes-Romero, F. Almonacid, M. Theristis, J. de la Casa, G. E. Georghiou, and E. F. Fernández, "Comparative analysis of parameter extraction techniques for the electrical characterization of multi-junction CPV and m-Si technologies," *Sol. Energy*, vol. 160, pp. 275–288, Jan. 2018, doi: 10.1016/j.solener.2017.12.011.

[33] J. Appelbaum and A. Peled, "Parameters extraction of solar cells—A comparative examination of three methods," *Sol. Energy Mater. Sol. Cells*, vol. 122, pp. 164–173, Mar. 2014, doi: 10.1016/j.solmat.2013.11.011.

[34] E. F. Fernández, J. Montes-Romero, J. de la Casa, P. Rodrigo, and F. Almonacid, "Comparative study of methods for the extraction of concentrator photovoltaic module parameters," *Sol. Energy*, vol. 137, pp. 413–423, Nov. 2016, doi: 10.1016/j.solener.2016.08.046.

[35] J. C. H. Phang, D. S. H. Chan, and J. R. Phillips, "Accurate analytical method for the extraction of solar cell model parameters," *Electron. Lett.*, vol. 20, no. 10, pp. 406–408, 1984, doi: 10.1049/el:19840281.

[36] M. A. de Blas, J. L. Torres, E. Prieto, and A. Garcıa, "Selecting a suitable model for characterizing photovoltaic devices," *Renew. Energy*, vol. 25, no. 3, pp. 371–380, Mar. 2002, doi: 10.1016/s0960-1481(01)00056-8.

[37] F. Khan, S.-H. Baek, Y. Park, and J. H. Kim, "Extraction of diode parameters of silicon solar cells under high illumination conditions," *Energy Convers. Manage.*, vol. 76, pp. 421–429, Dec. 2013, doi: 10.1016/j.enconman.2013.07.054.

[38] F. Almonacid, P. Rodrigo, and E. F. Fernández, "Determination of the current–voltage characteristics of concentrator systems by using different adapted conventional techniques," *Energy*, vol. 101, pp. 146–160, Apr. 2016, doi: 10.1016/j.energy.2016.01.082.

[39] L. E. P. Chenche, O. S. H. Mendoza, and E. P. B. Filho, "Comparison of four methods for parameter estimation of mono- and multi-junction photovoltaic devices using experimental data," *Renew. Sustain. Energy Rev.*, vol. 81, pp. 2823–2838, Jan. 2018, doi: 10.1016/j.rser.2017.06.089.

[40] W. Xiao, W. G. Dunford, and A. Capel, "A novel modeling method for photovoltaic cells," in *Proc. IEEE 35th Annu. Power Electron. Specialists Conf.*, Jun. 2004, pp. 1950–1956.

[41] N. S. Singh and A. Kapoor, "Determining multi-junction solar cell parameters using Lambert-W function," *Paripex Indian J. Res.*, vol. 3, no. 5, pp. 203–206, Jan. 2012, doi: 10.15373/22501991/may2014/62.

[42] F. F. Muhammadsharif, "A new simplified method for efficient extraction of solar cells and modules parameters from datasheet information," *Silicon*, vol. 14, no. 6, pp. 3059–3067, Apr. 2022, doi: 10.1007/s12633-021-01097-1.

[43] H. Rezk and A. Fathy, "A novel optimal parameters identification of triple-junction solar cell based on a recently meta-heuristic water cycle algorithm," *Sol. Energy*, vol. 157, pp. 778–791, Nov. 2017, doi: 10.1016/j.solener.2017.08.084.

[44] F. Ghani, E. F. Fernandez, F. Almonacid, and T. S. O'Donovan, "The numerical computation of lumped parameter values using the multi-dimensional Newton–Raphson method for the characterisation of a multi-junction CPV module using the five-parameter approach," *Sol. Energy*, vol. 149, pp. 302–313, Jun. 2017, doi: 10.1016/j.solener.2017.04.024.

[45] L. Nouri, F. Z. Ihfa, Y. A. Oubella, Z. Sakhi, and M. Bennai, "Single-diode multi-junction solar cell models five-parameter estimation method," *Indian J. Phys.*, vol. 98, no. 2, pp. 629–637, Feb. 2024, doi: 10.1007/s12648-023-02823-8.

[46] F. Belabbes, D. T. Cotfas, P. A. Cotfas, and M. Medles, "Using the snake optimization metaheuristic algorithms to extract the photovoltaic cells parameters," *Energy Convers. Manag.*, vol. 292, Sep. 2023, Art. no. 117373, doi: 10.1016/j.enconman.2023.117373.

[47] M. Abdel-Basset, D. El-Shahat, R. K. Chakrabortty, and M. Ryan, "Parameter estimation of photovoltaic models using an improved marine predators algorithm," *Energy Convers. Manage.*, vol. 227, Jan. 2021, Art. no. 113491, doi: 10.1016/j.enconman.2020.113491.

[48] W. Skelton, Y. Ji, L. Artzt, C. Spitler, G. Ingrish, K. Islam, D. Codd, and M. D. Escarra, "Design and field testing of a sunflower hybrid concentrator photovoltaic-thermal receiver," *Cell Rep. Phys. Sci.*, vol. 3, no. 5, May 2022, Art. no. 100887, doi: 10.1016/j.xcrp.2022.100887.

[49] A. O. M. Maka and T. S. O'Donovan, "Effect of thermal load on performance parameters of solar concentrating photovoltaic: High-efficiency solar cells," *Energy Built Environ.*, vol. 3, no. 2, pp. 201–209, Apr. 2022, doi: 10.1016/j.enbenv.2021.01.004.

[50] A. Abbassi, R. B. Mehrez, Y. Bensalem, R. Abbassi, M. Kchaou, M. Jemli, L. Abualigah, and M. Altalhi, "Improved arithmetic optimization algorithm for parameters extraction of photovoltaic solar cell single-diode model," *Arabian J. Sci. Eng.*, vol. 47, no. 8, pp. 10435–10451, Aug. 2022, doi: 10.1007/s13369-022-06605-y.

[51] V. Hayyolalam and A. A. P. Kazem, "Black widow optimization algorithm: A novel meta-heuristic approach for solving engineering optimization problems," *Eng. Appl. Artif. Intell.*, vol. 87, Jan. 2020, Art. no. 103249, doi: 10.1016/j.engappai.2019.103249.

[52] A. F. Peña-Delgado, H. Peraza-Vázquez, J. H. Almazán-Covarrubias, N. T. Cruz, P. M. García-Vite, A. B. Morales-Cepeda, and J. M. Ramirez-Arredondo, "A novel bio-inspired algorithm applied to selective harmonic elimination in a three-phase eleven-level inverter," *Math. Problems Eng.*, vol. 2020, pp. 1–10, Dec. 2020, doi: 10.1155/2020/8856040.

[53] M. Madhiarasan, D. T. Cotfas, and P. A. Cotfas, "Black widow optimization algorithm used to extract the parameters of photovoltaic cells and panels," *Mathematics*, vol. 11, no. 4, p. 967, Feb. 2023, doi: 10.3390/math11040967.

[54] M. S. Braik, "Chameleon swarm algorithm: A bio-inspired optimizer for solving engineering design problems," *Expert Syst. Appl.*, vol. 174, Jul. 2021, Art. no. 114685, doi: 10.1016/j.eswa.2021.114685.

[55] P. A. Cotfas and D. T. Cotfas, "Design and implementation of RELab system to study the solar and wind energy," *Measurement*, vol. 93, pp. 94–101, Nov. 2016, doi: 10.1016/j.measurement.2016.06.060.

[56] D. S. H. Chan, J. R. Phillips, and J. C. H. Phang, "A comparative study of extraction methods for solar cell model parameters," *Solid-State Electron.*, vol. 29, no. 3, pp. 329–337, Mar. 1986, doi: 10.1016/0038-1101(86)90212-1.

[57] CESI. (2020). *Thin Triple-Junction Solar Cell for Space Applications*. [Online]. Available: https://www.cesi.it/app/uploads/2020/03/Datasheet-CTJ30-Thin.pdf

DANIEL T. COTFAS was born in Toplita, Harghita, Romania, in 1970. He received the B.S. and M.S. degrees in mathematics and physics from the Transilvania University of Brasov, Romania, in 1995 and 2001, respectively, the Ph.D. degree, in 2008, and the Habilitation degree in electronic engineering, telecommunications and information technology, in 2019.

In 2002, he joined the Physics Department, Transilvania University of Brasov, as an Assistant, where he became a Lecturer, in 2004. In 2011, he joined the Electronics and Computers Department, Transilvania University of Brasov, where he became an Associate Professor, in 2015, and a Professor, in 2020. He is the author of 11 books and chapter books, and more than 100 articles. He holds one patent. His current research interests include renewable energy, energy harvesting, hybrid systems photovoltaic/thermoelectric/solar collector testing, optoelectronics, virtual instrumentation, and remote engineering.

Dr. Cotfas is a member of the International Association of Online Engineering (IAOE), the Physics Romanian Society (SRF), the European Optical Society (EOS), and the Leonardo Virtual Community. He won three awards at the Graphical System Design Achievement Awards from NIWeek 2013 with the Renewable Energy Laboratory Using NI ELVIS, NI LabVIEW, and NI myDAQ, and the Gold Medal from EUROINVENT, Iasi, Romania, in 2015. He is the guest editor of more journals. He is an Associate Editor of *International Journal of Photoenergy* and *Frontiers in Energy Research*.

MANOHARAN MADHIARASAN received the Bachelor of Engineering degree in electrical and electronics engineering from the Jaya Engineering College, Thiruninravur, under Anna University, Tamil Nadu, India, in 2010, the Master of Engineering degree in electrical drives and embedded control (electrical engineering) from Anna University, Regional Centre, Coimbatore, under Anna University, in 2013, and the Ph.D. degree in electrical engineering from Anna University, in 2018.

He was an Assistant Professor and a Research and Development In-Charge with the Department of Electrical and Electronics Engineering, Bharat Institute of Engineering and Technology, Hyderabad, India, from August 2018 to July 2020. He was a Postdoctoral Fellow with the Department of Computer Science and Engineering, Indian Institute of Technology Roorkee (IITR), India, from December 2020 to April 2022. He was a Postdoctoral Fellow with the Department of Electronics and Computers, Faculty of Electrical Engineering and Computer Science, Transilvania University of Brasov,

Romania, from May 2022 to April 2023. He was a Research and Development Coordinator and an Associate Professor with the Department of Electrical and Electronics Engineering, Dhanalakshmi Srinivasan College of Engineering and Technology, East Coast Road, Mamallapuram, Chennai, Kanchipuram, Tamil Nadu, from June 2023 to October 2023. His research interests include electrical engineering, renewable energy systems, power electronics and control, computer vision, human–computer interface, pattern recognition, artificial intelligence, neural networks, optimization, machine learning, deep learning, soft computing, the Internet of Things, and modeling and simulation.

Dr. Madhiarasan has been a technical program committee member, an international scientific committee member, and a keynote speaker at many international conferences. Furthermore, he received the UGC (RGNF) Fellowship, the prestigious Transilvania Fellowship for Postdoctoral Research/Young Researchers, and the Best Researcher Award from the 10th Edition of Global Research Awards on Artificial Intelligence and Robotics, in 2023. He presented his research work nationally and internationally. He served as the Publication Chair for the International Conference on Artificial Intelligence, Big Data and Mechatronics (AIBDM 2021). He acts as an Editorial Board Member and a Reviewer for many peer-reviewed international journals, such as Springer, Elsevier, IEEE Access, MDPI, and Hindawi, and the Lead Guest Editor of *Sensors* (MDPI), *Sustainability* (MDPI), *Applied Sciences* (MDPI), *Thermal Science and Engineering*, and *Energy Engineering*.

PETRU A. COTFAS (Member, IEEE) received the B.Sc. degree in mathematics and physics, in 1997, the M.Sc. degree in mathematics and computer science from the Transilvania University of Brasov, Romania, in 1998, the B.Sc. degree in computer science, in 2001, and the Ph.D. degree in material science engineering from the Transilvania University of Brasov, in 2007.

He is currently a Full Professor with the Electronics and Computers Department, Transilvania University of Brasov. Having vast experience in the fields of photovoltaics and hybrid systems characterization and testing, virtual instrumentation, data acquisition, graphical programming, and remote engineering, he published ten books or chapter books in national and international publishing houses and more than 140 papers in international and national journals and conferences proceedings.

Dr. Cotfas is a member of the International Association of Online Engineering and the Romanian Physical Society. He received three awards at the World Contest Graphical System Design Achievement Award organized by National Instruments, Austin, TX, USA, in 2013, for the Renewable Energy Laboratory (RELab) Board Development and the associated case study. The RELab Board was also awarded a Gold Medal at the International Salon of Inventions-EUROINVENT 2015, Iasi, Romania.